

We thank the two anonymous referees for their insightful comments to the manuscript and helpful suggestions for improving the presentation quality. Below, we explain how the comments and suggestions are addressed (our point-by-point responses in blue) and make note of the changes we have made to the discussion paper, attempting to take into account all the comments raised by both referees.

## **Referee #1**

This paper presents the results of a one-year's model simulation of black carbon aerosols over the Tibetan Plateau. The authors use NCAR's CAM5 model, implemented with a source tagging technique, to quantify the BC over different regions of the Tibetan Plateau from various geographical regions (the surrounding areas in particular) and two major source sectors (biofuel/biomass and fossil fuel). They also characterize the seasonal variations of BC concentrations, deposition and radiative forcing on the plateau as well as their source attribution, and analyze the model results in very detail. The paper is interesting and should be a welcome addition to the literature. I would suggest the paper to be published after the following questions/comments have been well addressed.

### **General comments:**

1) The tagging method used in this study is not well introduced. Although the title of Sect. 2.1 is written to comprise “the source-tagging method”, no content related to the method can be found in this subsection at all. In Sect. 2.2, several equations are given, but these equations are far away from the model tagging technique. The authors refer to Wang et al. (2014) for the source-receptor relationships. However, only the similar equations were presented in that work. I would suggest that the authors give much more detailed description about the treatment of BC in CAM5, especially the tagging method. For example, in which aerosol modes BC are taken into account? Are they all assumed to be hygroscopic and internally-mixed? How many tracers are added in the model to tag the BC from a specific region? Is there a tracer added for each mode? Is there a tracer for BC in snow? Is the tagged BC assumed to undergo the same dynamic and microphysical processes as the normal BC does in the model? Perhaps, you do not need adding a tracer to tag the BC, but it should be described clearly how to achieve that.

Response: CAM5 employs a modal aerosol module (MAM) to represent aerosols in multiple log-normally distributed modes, with internal mixing assumed for aerosol species within each individual mode, including a 3-mode standard representation (MAM3) and a more complex 7-mode representation (MAM7). The major difference between MAM3 and MAM7 related to carbonaceous aerosols lies in the treatment of aging. In MAM3, black carbon (BC) and primary organic matter (POM) are emitted

into the accumulation mode that contains highly hygroscopic species such as sulfate and sea-salt, while in MAM7 BC and POM are emitted into a primary carbon mode, which contains no other species. BC is hydrophobic upon emission, and thus the hygroscopicity of the primary carbon mode depends on the assumed hygroscopicity for POM. As hygroscopic species condense onto the primary-carbon-mode particles, the particles are become more hygroscopic and are transferred into the MAM7 accumulation mode. The rate of transfer is controlled by uncertain aging parameters, and the availability of gas precursors (Liu et al. 2012).

In this study, we apply the direct source tagging technique developed by Wang et al. (2014) to the accumulation-mode BC in the MAM3 treatment. BC particles emitted from sixteen geographical BC source regions and two emissions sectors (i.e., biomass burning & biofuel emissions and fossil fuel emissions) in each of the regions are tagged and explicitly tracked. Instead of using the global emissions from all sectors for the original one BC variable, the thirty two regional/sectoral emissions provide sources to the respective tagged BC mass mixing ratio variables that are all added to the accumulation mode, including both interstitial and cloud-borne states. All physical and dynamic tendencies (e.g., transport, dry and wet removal) are calculated explicitly for the tagged BC variables in the same way as the original BC mass mixing ratios. Also, when aerosol optical properties are calculated, all of the tagged BC mass mixing ratios contribute to the volume-mean refractive index of the accumulation mode that is used in the radiation calculation.

We have now added such detailed descriptions to the revised manuscript.

2) While the paper focuses mainly on the quantification of the contributions to BC on the Tibetan Plateau from different source regions, the analysis of various physical processes is relatively weak. It is stated that the study is to “characterize the fate of BC particles emitted from various geographical regions” in both the Abstract and Conclusions. However, the lifetimes of BC from different regions are not investigated as expected. With the definition given in Page 86 (the equation should be numbered), the authors investigate the efficiency of tagged sources in affecting the BC on the Tibetan Plateau (Fig. 7). In addition to the geographical distance or atmospheric transport pathway between the receptor and a source region, are there any other factors (e.g., aerosol chemistry, microphysical processes and dry/wet deposition) affect the estimated efficiency?

Response: The main focus points of this paper do not include the analysis of various physical processes that contribute to aerosol removal and lifetime in CAM5, which have been extensively evaluated in previous studies (e.g., Wang et al., 2013, 2014), including the aging, wet deposition, and lifetime of regional BC. However, to address

the referee's concern, here we calculate the annual and seasonal mean lifetime of BC from different geographical regions and sectors. These results are summarized in Table R1. On the globe average, BB BC has a longer lifetime than FF BC in all seasons, especially in winter (6.9 vs. 3.1 day), which is likely because biomass burning emissions in the BB category have initial injection heights of up to 6 km, resulting in less removal at lower altitudes. The availability of co-emitted hygroscopic species (in the same accumulation mode of the MAM3 aerosol treatment) also impacts the scavenging and wet removal rate of BC. This also partly explains the variability of lifetime of BC originating from the different source regions and sectors. Regarding the seasonal cycle, BC emitted from the major source regions (e.g., SAF, EAS, SEA, SAS) has substantially lower lifetime in summer (JJA) than in the other seasons, likely due to relatively strong removal by summer monsoon precipitation. The table has been included in the Supplement (Table S2) and the main message is summarized in the paper.

According to its definition in Eq. 2 (now numbered), the efficiency can be affected by regional emission rate and factors that influence the amount of BC emitted from the specific source region reaching the receptor region (i.e., HTP). The main factors are the transport pathway determined by large-scale circulations and convective lifting and dry/wet removal rate during the transport that is determined by aerosol properties, aerosol microphysics, and cloud microphysical processes. These processes are all represented in the prognostic equation for aerosols. We just did not focus on analyzing the individual budget terms in this study.

Table R1. Global annual and seasonal mean lifetime (day) of BC emitted from the 32 tagged source regions/sectors, as well as from BB and FF sector over the whole globe (all source regions combined).

		<b>DJF</b>	<b>MAM</b>	<b>JJA</b>	<b>SON</b>	<b>ANN</b>
<b>ARC</b>	BB	2.2	3.0	4.7	3.9	4.5
	FF	2.1	1.9	1.6	1.4	1.7
<b>NAM</b>	BB	2.2	3.0	4.1	3.6	3.4
	FF	2.1	2.8	3.9	3.2	3.0
<b>CAM</b>	BB	2.6	4.9	2.8	1.7	3.9
	FF	3.5	5.0	2.4	2.3	3.3
<b>SAM</b>	BB	3.5	3.7	8.4	6.8	6.8
	FF	2.9	3.0	4.1	3.9	3.5
<b>EUR</b>	BB	2.0	2.7	6.4	4.0	4.0
	FF	1.9	2.5	4.9	2.9	3.1
<b>NAF</b>	BB	8.8	10.8	10.2	10.0	10.0
	FF	5.4	8.9	12.9	9.1	9.1

<b>SAF</b>	BB	9.3	6.1	5.1	7.1	7.2
	FF	4.4	4.1	4.3	3.9	4.2
<b>MDE</b>	BB	5.9	8.9	12.6	11.3	9.9
	FF	6.2	9.1	12.4	11.5	9.8
<b>CAS</b>	BB	2.8	4.7	7.5	4.7	5.9
	FF	2.7	5.4	9.7	5.8	5.9
<b>SAS</b>	BB	7.4	7.5	1.9	4.4	5.5
	FF	7.5	7.6	2.3	4.9	5.6
<b>EAS</b>	BB	3.2	3.6	2.5	3.1	3.1
	FF	3.1	3.3	2.4	3.0	2.9
<b>SEA</b>	BB	2.7	3.5	1.8	1.8	2.5
	FF	2.2	1.8	1.4	1.5	1.7
<b>PAN</b>	BB	5.7	4.5	5.6	6.8	6.1
	FF	4.2	3.3	2.5	2.9	3.2
<b>RBU</b>	BB	2.2	3.8	4.4	3.4	4.0
	FF	2.0	2.5	4.9	2.6	3.0
<b>HTP</b>	BB	6.6	6.0	4.0	6.5	5.8
	FF	6.1	6.2	4.9	6.4	5.9
<b>ROW</b>	BB	2.2	2.6	4.1	2.7	2.9
	FF	2.3	2.5	2.4	2.5	2.5
<b>Globe</b>	BB	6.9	5.0	4.6	5.2	5.4
	FF	3.1	3.6	3.8	3.5	3.5

3) Comparisons with previous studies, e.g. the work of Kopacz et al. (2011) and Lu et al. (2012), are not sufficient in the current version of the paper. What advantages and limitations of the methods used in these studies, where the same topic are addressed?

Are there any disagreements or uncertainties for the BC source contributions and radiative forcing over the Tibetan Plateau based on these studies?

Response: Kopacz et al. (2011) employed a global chemical transport model, GEOS-Chem, and its adjoint to identify the originating locations of BC arriving at five glacier sites (i.e., five model grid-cells as the receptors) in the Himalayas and Tibetan Plateau (HTP) in year 2001. This method can provide a global distribution of emissions that directly contribute to BC concentrations at receptor locations. While the adjoint model accounts for nonlinearities in the relationships between aerosols and emissions, the results are still merely tangent linear derivatives (gradients). In contrast to our source tagging approach, the adjoint model results are not source attributions but rather the source-receptor sensitivities, which can be interpreted as the effectiveness of incremental changes to existing emissions. Our direct tagging method



can attribute sources to predefined geographical regions as well as emission sectors. While the adjoint approach has the advantage of not predefining source regions, it does need to perform simulations for each defined receptor region. Our tagging method also has the flexibility to do source attribution of BC mass mixing ratio at any model layer and the surface dry/wet deposition within a single simulation for any receptor regions.

Lu et al. (2012) used an improved back-trajectory approach to analyze the origin of BC transported to the HTP during 1996-2010. Based on a large set of seven-day back trajectories arriving at the given receptor locations in the HTP, BC emissions, and transport efficiencies (representing the transport ability of BC from source to receptor by taking into account advection, aging and removal processes of BC), they derived the overall transport characteristics of BC to the HTP and showed the spatial distribution of sources for BC reaching the HTP region. The statistical analysis of trajectories has good accuracy on short time scales for source regions with close proximity to the receptor, but this approach has limitations in determining contributions from distant sources. The seven-day back trajectories (spanning the average BC lifetime) might be sufficient to characterize the source origins of air masses arriving at the boundary layer of HTP (e.g., 500 m arrival height in Lu et al.'s study), but are probably not adequate for BC being transported in the mid- and upper-troposphere that could contribute significantly to the total column burden but less to BC deposition and boundary layer concentrations.

With the different approaches, Kopacz et al. (2011), Lu et al. (2012) and the present study all show that South Asia and East Asia are the main source regions for BC transported to the HTP, while the magnitude of contributions from each of the source regions varies with season and receptor location. Although all of the three studies can provide quantitative contributions of emissions from the various source regions to BC in the HTP, a quantitative inter-comparison of the findings is quite difficult, given the differences in the definition of geographical source/receptor regions, emission inventories, time periods for model simulation, and analysis methods. Nevertheless, in addition to quantifying the contributions of source regions, our direct source tagging approach allows us to further break down regional contributions to sectors (i.e., fossil fuel vs. biomass & biofuel) and to characterize the transport pathways of individual regional/sectoral emissions. Compared to the way we calculated the spatial and temporal mean BC radiative forcing (in both the atmosphere and snow), Kopacz et al (2011) did offline calculations of instantaneous radiative forcing in the snow-covered regions only, while Lu et al. (2012) did not include any radiative forcing calculations. In addition, we also did source attributions for BC-in-snow forcing.

We have added a summary of the response here to the manuscript.

## Referee #2

### General comments:

The results provide an interesting way to view the relatively pristine HTP that is embedded among major carbon emissions hot spots. My comments reflect a general critique that the authors do not sufficiently motivate the finer points of the discussion. The most confusing points are related to efficiency and finer source-receptor relationships within the HTP, and I think these need clarification before the paper should be published. Otherwise, there are some very interesting emissions impacts results on a very sensitive part of the world (ie. the Third Pole). Figure 4 is fascinating!

There is some repetition in the first 200 lines of text that I would recommend streamlining. One way to do this would be to clarify why some of the studies are mentioned in this study. Bring their relevance to the foreground.

I have some issues trying to understand the utility of the efficiency metric that I think may require some further discussion by the authors before the paper should be published. My recommendation is that the entire efficiency discussion be deleted – it seems underdeveloped and seems to not support the main points of the paper. I also note, however, that I may have misunderstood the calculation, but either way, I requested a direct response to this.

Also, the source-receptor relationships within the HTP are interesting, but I do not understand why I am reading about them.

Response: Thanks for the general comments and suggestions. We have now made changes to the introduction section according to the specific suggestions below and other changes to streamline the flow. Regarding the use of the efficiency metric and why we further divide the HTP into five finer receptor regions, please see our responses to the same but more specific comments below.

### Specific Comments:

Line 100: Citation for sentence starting with “A large fraction . . .”? Could this be better quantified to say approximately what fraction?

Response: changed to “Over 60% of BC in the present-day atmosphere originates from anthropogenic activities (e.g., Bond et al., 2007; Lamarque et al., 2010)”

Line 102: “Road map” is an odd choice of words for this study. Perhaps just be more specific and less flowery about what makes some scientists think that BC mitigation is a low-hanging fruit.

Response: changed “manage the road map of climate forcing” to “slow down the climate change”

Line 159: Repetitive with line 117. I recommend deleting one and adding to the one that remains in the text a preview of why this study is highlighted in your study (ie. as a basis of comparison about source regions of BC as cited later in the manuscript).

Response: deleted the repetitive sentence in line 159 and added more context near line 117 to explain why Kopacz et al. (2011) is highlighted in the present study. Please also see our response to comment #3 of referee #1 regarding a more detailed comparison between our study and two other ones including Kopacz et al. (2011).

Line 165: What do you mean by “different inventories” since I’m only aware of the CMIP5 inventories, and this is the only one cited?

Response: We meant that there are “top-down” and “bottom-up” global emission inventories, and some emission data sets like the ECLIPSE include newly identified emissions from gas flaring and residential heating at high-latitudes. To avoid such confusion, we have deleted the sentence “BC emission datasets have large uncertainties (e.g., Bond et al., 2013), and there are different inventories available for climate modeling.”

Line 173-174: I don’t understand. Why is a ratio of biofuel to fossil fuel needed? Doesn’t Lamarque et al (2010) emissions include a biofuel category? If not, maybe simply stating that this is why a ratio is needed would be clearer.

Response: Lamarque et al. (2010) doesn’t directly provide biofuel and fossil fuel BC emission sectors, so we need a ratio of biofuel to fossil fuel. This has now been clarified in the text.

Line 200, 203: Does mass mixing ratio, deposition flux, surface mixing ratio as a BC property produce similar results as using column burden? It seems like MMR C value would be much different than column burden, unless this is a z-dependent C calculation. Either way, and similar to other comments, introducing this myriad of metrics is interesting, but it would be helpful to clarify why they are all needed. For example, are C values for MMR and SMR even discussed in this study? From Fig 6, I see deposition and column burden C values.

Response: The referee is correct that the relative contribution by a specific source could be significantly different between the BC column burden and mass mixing ratio (MMR) at a certain height (e.g., near the surface). The model simulated surface MMR is often compared to observations made at surface stations for model evaluation. For example, we did such a comparison in Figure 2. In Figure 4, we use BC vertical distributions to illustrate its transport pathways on the latitude-height cross-section.

The direct source tagging approach does enable us to do BC source attribution at any height (or model pressure level) in addition to that for the total column burden and deposition flux, and thus it is more flexible than the other approaches employed in previous studies (e.g., Kopacz et al., 2011; Lu et al. 2012). The total column burden is more relevant to the calculation of atmospheric BC radiative forcing, while the deposition flux largely determines BC-in-snow radiative forcing. Therefore, the source attributions for these two properties are presented in the paper (e.g., Figure 6). Although the source attribution of BC at the surface or any given height is not the focus of this study, we believe this capability is worth noting when introducing the metrics here.

Line 261: What emission uncertainties? Are these quantified in a peer-reviewed source?

Response: Using bottom-up inventory methods, Bond et al (2013) estimated an uncertainty range of 2 to 29 Tg yr<sup>-1</sup> along with a best estimate of about 7.5 Tg yr<sup>-1</sup> for the global BC emissions in year 2000. Cohen and Wang (2014) derived an optimized top-down estimate of global BC emissions,  $17.8 \pm 5.6$  Tg yr<sup>-1</sup>, a factor of two higher than commonly used global BC emissions. We have added a reference to this in the paper.

Line 285: Can this improvement for HTP be quantified in some way? The discussion around CAM5 simulated SCF and MODIS SCF uncertainty is muddled and missing a simpler metric of comparison. For example, the average correlation of the SCF in the study area for CAM5 vs MODIS 2001 and MODIS 2000-2013 should be illustrative. What is the average SCF in each season for the different comparisons? Can the improvement from CAM3 to CAM5 be better quantified beyond the citation to Qian et al. 2011? As it is, it's not very convincing to read about dramatic improvements without a number.

Response: Following the referee's suggestion, we have now calculated the correlation coefficient of SCF between CAM5 and MODIS and performed the statistical significance test (see Table R2). There are a total number of 52 model grid-cells over the HTP, and note that MODIS retrievals were mapped to the CAM5 grid. It shows that the CAM5 SCF is highly correlated with that of MODIS (both 2001 and 2000-2013) with the statistical confidence level greater than 99%, except for summer (JJA) when the linear correlation is significant only at 80% level. The results have been added to the paper.

We have also calculated the annual and seasonal mean SCF over the HTP for CAM5 and MODIS and added the numbers to the corresponding panels in Figure 3. The standard deviation of the MODIS SCF climatology, which indicates intra-seasonal

and inter-annual variations, is also calculated based on monthly mean SCF during 2000-2013.

The CAM3 model used by Qian et al. (2011) overestimates SCF by 20-100% during the cold season (November to April). The CAM3 spring (MAM) mean SCF is greater than 35%, while the CAM5 SCF (21%) in the present study that is in good agreement with the MODIS SCF (18±5%). We have added the quantitative comparison to the paper.

Table R2: Correlation coefficient ( $R$ ) and its statistical significance ( $p$ ) of SCF between CAM5 and MODIS

	CAM5 (2001) vs. MODIS (2001)		CAM5 (2001) vs. MODIS (2000-2013)	
	$R$	$p$	$R$	$p$
DJF	0.61	0.00000	0.61	0.00000
MAM	0.76	0.00000	0.83	0.00000
JJA	0.17	0.22496	0.18	0.20823
SON	0.88	0.00000	0.82	0.00000
ANN	0.78	0.00000	0.80	0.00000

Line 294: What is the mean SCF? This is never stated, and “very close” is too vague.

Response: The DJF mean SCF is 50%, which is now added to the text and also shown in the revised Figure 3. The “very close” wording has been removed.

Line 306, Figure 4: This is a very complex graphic, but I think very useful, provided some revisions are made to both the figure and the manuscript text. The figure either should be larger or broken into multiple parts. I think larger would work well given that the orientation of the figure currently does a great job with side-by-side comparisons of source regions impacts on HTP as a function of two seasons. The wind vectors right now are very challenging to read, but maybe a larger figure solves this? Also, somewhere, it should be stated why these 6 source regions were selected from the 16 on Fig 1. This is mentioned on Line 306 (“six major source regions”) but I would think that RBU would have some seasonal impact, especially during JJA when fire activity is high. I do not have the supplemental figures in my version of the manuscript, so I could not judge this.

Response: As the referee has correctly pointed out, the main reason to place the DJF and JJA panels in the same figure is for side-by-side comparisons. Also, the figure was designed to occupy a whole page for the portrait layout of final ACP publication,

which we will work on with the production editor at the typesetting stage.

The six source regions shown in the figure were identified according to the annual mean contributions. However, the referee is correct that RBU has a larger seasonal contribution (during JJA) than SAF. This has now been discussed in the text (Sect. 4.3). Sorry that the supplemental figures were not appended to the manuscript, but they are in a separate file that has a link on the webpage for the manuscript.

Line 328: This caveat (no seasonality in FF) should be discussed when talking about what FF means in Section 2.2.

Response: We have added a sentence in Section 2.2: “Note that emissions in the BB sector have seasonal variations, but the FF sector emissions used in this study have no seasonal variation at all.”

Line 334-337: This text would benefit from referencing your own Fig. 4

Response: added reference to Fig. 4 in the text.

Line 377, Section 4.3: This is a key section, but missing from the discussion as to why HTP is broken into multiple source regions. I expected to see this discussion before the conclusion (see my comment line 578) but nothing appeared. To me, the more interesting points of this study are the source-receptor analysis of HTP as a whole. Why should I be interested in more detail? What are the ramifications?

Response: As shown in Figure 2, both modeled and observed near-surface BC concentrations at different sampling site locations over the HTP have quite different seasonal mean values and variations. Model simulated seasonal BC column burden and deposition flux also vary with location on the HTP (Figure 4). Snow cover over HTP also has large spatial variability (see Figure 3). As a result, the annual and seasonal mean BC radiative forcings (in both the atmosphere and snow) vary significantly with location (Figure 8). We intend to quantify source contributions to BC in each of the sub-regions over the HTP. It turned out that the source-receptor relationships for BC burden, deposition and radiative forcing have large spatial variability as well (Figures 6 and 8). We believe this is more interesting than focusing on the HTP region as a whole. The HTP contains a large number of glaciers that distribute at many different locations (e.g., Figure 1 in Yao et al., 2012). Many studies have suggested that the BC in snow/ice may be partly responsible for the observed acceleration of glacier retreat in the HTP. The BC source attribution information for finer regions will be of more interest to researchers using ice-core BC retrievals at individual glaciers. Kopacz et al (2011) used the GEOS-Chem model and its adjoint to identify the originating locations of BC arriving at five glacier sampling sites in the HTP, even though they needed to perform simulations separately for each of the sites.

They also found that the magnitude of the contribution from each source region varies strongly with receptor locations (e.g., sampling sites). Our explicit source tagging method has the advantage of doing source attribution of BC for any receptor regions without rerunning the model simulation. Therefore, it is scientifically important and technically efficient to perform the source-receptor analysis for the HTP not only as a single receptor but also as multiple finer receptors.

We have now added this motivation in the paper.

Line 459: Perhaps I have misunderstood this efficiency metric, but here is where I stand on this and I would appreciate a defense/clarification: Section 4.4 seems unnecessary to support the main points of the study. I do not see how this efficiency metric is of much use, especially for HTP. HTP has practically no emissions and I do not see how anyone could practically expect HTP to develop major emission sources. SAS and EAS have enormous emissions. To standardize to present day emissions seems to minimize the impact of the largest emitters on HTP at least. In other words, all this efficiency metric highlights is that the S values in line 207 are divided by a very very small number. To make a more effective efficiency metric, wouldn't all emissions have to be uniform across the globe and source region perturbations of equal magnitude be applied to study the actual efficiency at which an equivalent emissions increase would have on a receptor region? Again, pardon any misunderstanding if I have missed something.

Response: The fractional contribution metric helps quantify the relative importance of individual source regions/sectors in affecting BC over the HTP and estimate the response to percentage change in sources, while the efficiency metric is more useful to characterize the sensitivity of BC in the receptor to absolute change (or per-mass perturbation) in regional/sectoral emissions. If the emissions were uniformly distributed over the globe as the referee suggested, the efficiency metric would be equivalent to the contribution metric. Because the efficiency is essentially the contribution normalized by emission strength, it is less dependent on emission rate in source regions than on removal processes and transport. The referee is correct that we mean to use the efficiency metric to measure the impact of equal magnitude of perturbations in different source regions on BC in the receptor region. Although the HTP local emissions are very minimal (see Figure 1b), their contribution to BC burden and deposition at all of the sub-regions is quite significant, even comparable to East Asia's in some of the regions (see Figure 6). In other words, the efficiency of local emissions in affecting HTP BC is very high (Figure 8), which means that the impact of per-unit-mass (or equal-magnitude) perturbation in emissions on BC over HTP is much stronger if the perturbation occurs within HTP than in any other source regions including SAS and EAS. Certainly, this metric is also useful for comparison

between other source regions and different seasons.

The efficiency metric is of more interest to policy makers for the purpose of mitigation action, which is not the focus of this study but is definitely worth mentioning. Therefore, we only use one figure and a sub-section to describe it, and we would like to keep it in the paper.

Line 565: This is a very clear summary of what I think are the key results – nicely written!

Response: Thanks!

Line 578: Similar to Line 377, can text be added to this paragraph clarifying why this regional receptor analysis is generally important? Otherwise, I would suggest eliminating this paragraph from the Conclusions section.

Response: please see the response to the line 377 comment above. We have now added a sentence here to clarify this.

## References:

- Bond, T. C., Bhardwaj, E., Dong, R., Jogani, R., Jung, S., Roden, C., Streets, D. G., and Trautmann, N. M.: Historical emissions of black and organic carbon aerosol from energy-related combustion, 1850–2000, *Global Biogeochem. Cy.*, 21, GB2018, doi:10.1029/2006GB002840, 2007.
- Bond, T. C., Doherty, S. J., Fahey, D. W., Forster, P. M., Berntsen, T., DeAngelo, B. J., Flanner, M. G., Ghan, S., Kärcher, B., Koch, D., Kinne, S., Kondo, Y., Quinn, P. K., Sarofim, M. C., Schultz, M. G., Schulz, M., Venkataraman, C., Zhang, H., Zhang, S., Bellouin, N., Guttikunda, S. K., Hopke, P. K., Jacobson, M. Z., Kaiser, J. W., Klimont, Z., Lohmann, U., Schwarz, J. P., Shindell, D., Storelvmo, T., Warren, S. G., and Zender, C. S.: Bounding the role of black carbon in the climate system: A scientific assessment, *J. Geophys. Res.-Atmos.*, 118, 5380–5552, doi:10.1002/jgrd.50171, 2013.
- Cohen, J. B., and Wang C.: Estimating global black carbon emissions using a top-down Kalman Filter approach, *J. Geophys. Res. - Atmos.*, 119, 307–323, doi:10.1002/2013JD019912, 2014.
- Kopacz, M., Mauzerall, D. L., Wang, J., Leibensperger, E. M., Henze, D. K., and Singh, K.: Origin and radiative forcing of black carbon transported to the Himalayas and Tibetan Plateau, *Atmos. Chem. Phys.*, 11, 2837–2852, doi:10.5194/acp-11-2837-2011, 2011.
- Lamarque, J.-F., Bond, T. C., Eyring, V., Granier, C., Heil, A., Klimont, Z., Lee, D., Liousse, C., Mieville, A., Owen, B., Schultz, M. G., Shindell, D., Smith, S. J., Stehfest, E., Van Aardenne, J., Cooper, O. R., Kainuma, M., Mahowald, N., McConnell, J. R., Naik, V., Riahi, K., and van Vuuren, D. P.: Historical (1850–2000) gridded anthropogenic and biomass burning emissions of reactive gases and aerosols: methodology and application, *Atmos. Chem. Phys.*, 10, 7017–7039, doi:10.5194/acp-10-7017-2010, 2010.
- Liu, X., Easter, R. C., Ghan, S. J., Zaveri, R., Rasch, P., Shi, X., Lamarque, J.-F., Gettelman, A., Morrison, H., Vitt, F., Conley, A., Park, S., Neale, R., Hannay, C., Ekman, A. M. L., Hess, P., Mahowald, N., Collins, W., Iacono, M. J., Bretherton, C. S., Flanner, M. G., and Mitchell, D.:



- Toward a minimal representation of aerosols in climate models: description and evaluation in the Community Atmosphere Model CAM5, *Geosci. Model Dev.*, 5, 709–739, doi:10.5194/gmd-5-709-2012, 2012.
- Lu, Z., Streets, D. G., Zhang, Q., and Wang, S.: A novel back-trajectory analysis of the origin of black carbon transported to the Himalayas and Tibetan Plateau during 1996–2010, *Geophys. Res. Lett.*, 39, L01809, doi:10.1029/2011GL049903, 2012.
- Qian, Y., Flanner, M. G., Leung, L. R., and Wang, W.: Sensitivity studies on the impacts of Tibetan Plateau snowpack pollution on the Asian hydrological cycle and monsoon climate, *Atmos. Chem. Phys.*, 11, 1929–1948, doi:10.5194/acp-11-1929-2011, 2011.
- Wang, H., Easter, R. C., Rasch, P. J., Wang, M., Liu, X., Ghan, S. J., Qian, Y., Yoon, J.-H., Ma, P.-L., and Vinoj, V.: Sensitivity of remote aerosol distributions to representation of cloud–aerosol interactions in a global climate model, *Geosci. Model Dev.*, 6, 765–782, doi:10.5194/gmd-6-765-2013, 2013.
- Wang, H., Rasch, P. J., Easter, R. C., Singh, B., Zhang, R., Ma, P. L., Qian, Y., and Beagley, N.: Using an explicit emission tagging method in global modeling of source-receptor relationships for black carbon in the Arctic: Variations, Sources and Transport pathways, *J. Geophys. Res.-Atmos.*, 119, 12888–12909, doi: 10.1002/2014JD022297, 2014.
- Yao, T., Thompson, L., Yang, W., Yu, W., Gao, Y., Guo, X., Yang, X., Duan, K., Zhao, H., Xu, B., Pu, J., Lu, A., Xiang, Y., Kattel, D. B., and Joswiak, D.: Different glacier status with atmospheric circulations in Tibetan Plateau and surroundings, *Nat. Clim. Change*, 2, 663–667, doi:10.1038/nclimate1580, 2012.

# **Quantifying sources, transport, deposition and radiative forcing of black carbon over the Himalayas and Tibetan Plateau**

Rudong Zhang<sup>1, 2, 3</sup>, Hailong Wang<sup>2</sup>, Yun Qian<sup>2</sup>, Philip J. Rasch<sup>2</sup>, Richard C. Easter<sup>2</sup>, Po-Lun Ma<sup>2</sup>, Balwinder Singh<sup>2</sup>, Jianping Huang<sup>1</sup>, and Qiang Fu<sup>1, 3</sup>

<sup>1</sup> Key Laboratory for Semi-Arid Climate Change of the Ministry of Education, College of Atmospheric Sciences, Lanzhou University, Lanzhou 730000, Gansu, China.

<sup>2</sup> Atmospheric Sciences and Global Change Division, Pacific Northwest National Laboratory (PNNL), Richland, WA 99352, USA.

<sup>3</sup> Department of Atmospheric Sciences, Box 351640, University of Washington, Seattle, WA 98195, USA.

Manuscript for submission to *Atmospheric Chemistry and Physics*

Correspondence to: Hailong.Wang@pnnl.gov

## Abstract

Black carbon (BC) particles over the Himalayas and Tibetan Plateau (HTP), both airborne and those deposited on snow, have been shown to affect snowmelt and glacier retreat. Since BC over the HTP may originate from a variety of geographical regions and emission sectors, it is essential to quantify the source-receptor relationships of BC in order to understand the contributions of natural and anthropogenic emissions and provide guidance for potential mitigation actions. In this study, we use the Community Atmosphere Model version 5 (CAM5) with a newly developed source tagging technique, nudged towards the MERRA meteorological reanalysis, to characterize the fate of BC particles emitted from various geographical regions and sectors. Evaluated against observations over the HTP and surrounding regions, the model simulation shows a good agreement in the seasonal variation of the near-surface airborne BC concentrations, providing confidence to use this modeling framework for characterizing BC source-receptor relationships. Our analysis shows that the relative contributions from different geographical regions and source sectors depend on season and location in the HTP. The largest contribution to annual mean BC burden and surface deposition in the entire HTP region is from biofuel and biomass (BB) emissions in South Asia, followed by fossil fuel (FF) emissions from South Asia, then FF from East Asia. The same roles hold for all the seasonal means except for the summer when East Asia FF becomes more important. For finer receptor regions of interest, South Asia BB and FF have the largest impact on BC in Himalayas and Central Tibetan Plateau, while East Asia FF and BB contribute the most to Northeast Plateau in all seasons and Southeast Plateau in the summer. Central Asia and Middle East FF emissions have relatively more important contributions to BC reaching Northwest Plateau, especially in the summer. Although local emissions only contribute about 10% of BC in the HTP, this contribution is extremely sensitive

Hailong Wang 4/14/2015 6:00 PM

Deleted: s

Hailong Wang 4/15/2015 1:07 AM

Deleted: the

Hailong Wang 4/14/2015 6:00 PM

Deleted: s

27 to local emission changes. Lastly, we show that the annual mean radiative forcing ( $0.42 \text{ W m}^{-2}$ )  
 28 due to BC in snow outweighs the BC dimming effect ( $-0.3 \text{ W m}^{-2}$ ) at the surface over the HTP.  
 29 We also find strong seasonal and spatial variation with a peak value of  $5 \text{ W m}^{-2}$  in the spring  
 30 over Northwest Plateau. Such a large forcing of BC in snow is sufficient to cause earlier snow  
 31 melting and potentially contribute to the acceleration of glacier retreat.

32

### 33 1 Introduction

34 Black carbon (BC) is a distinct type of carbonaceous particulate matter mainly emitted from the  
 35 incomplete combustion of fossil fuels, biofuels and biomass burning. It is the dominant insoluble  
 36 light-absorbing particulate species, both in the atmosphere and after deposition on snow and ice.  
 37 In addition to its impact on air quality, BC plays a unique and important role in the climate  
 38 system through its effect on radiation, clouds and snow albedo, and associated feedbacks that  
 39 modify atmospheric circulation patterns and/or accelerate the snowmelt and glacier retreat in the  
 40 Arctic and across the mid-latitudes of the northern hemisphere (Bond et al., 2013).

41 Modeling studies (e.g., Hansen et al., 2005; Qian et al., 2011) indicate that the climate  
 42 efficacy of BC in snow is much greater than efficacy of carbon dioxide or other anthropogenic  
 43 forcers, owing to a sequence of positive feedback mechanisms (Warren and Wiscombe, 1980,  
 44 1985; Conway et al., 1996; Hansen and Nazarenko, 2004; Jacobson, 2004; Flanner et al., 2007;  
 45 Ye et al., 2012; Hadley and Kirchstetter, 2012; Doherty et al., 2014). Flanner et al. (2009)  
 46 demonstrated that the global annual BC snow-albedo effect (darkening) outweighs the aerosol  
 47 (BC and organic matter) dimming effect (i.e., reduced the downwelling irradiance reaching the  
 48 surface) by a factor of about 6. The snow/ice-covered Himalayas and Tibetan Plateau (HTP)  
 49 region is more prone to these BC effects than other regions because of the surrounding two major

- Hailong Wang 4/5/2015 2:27 PM  
**Deleted:** BC-radiation interactions, BC-cloud interactions,
- Hailong Wang 4/5/2015 2:27 PM  
**Deleted:** BC
- Hailong Wang 4/5/2015 2:27 PM  
**Deleted:** -
- Hailong Wang 4/5/2015 2:27 PM  
**Deleted:** effect
- Hailong Wang 4/5/2015 2:28 PM  
**Deleted:** both
- Hailong Wang 4/5/2015 2:30 PM  
**Deleted:** results
- Hailong Wang 4/5/2015 2:39 PM  
**Deleted:** (Hansen et al., 2005)
- Hailong Wang 4/5/2015 2:39 PM  
**Deleted:** Model simulations also
- Hailong Wang 4/5/2015 2:41 PM  
**Deleted:** over global snow cover (Flanner et al., 2009)
- Hailong Wang 4/5/2015 2:43 PM  
**Deleted:** - and/or glacier
- Hailong Wang 4/5/2015 2:44 PM  
**Deleted:** regions such as the
- Hailong Wang 4/12/2015 10:56 PM  
**Deleted:** are
- Hailong Wang 4/12/2015 10:57 PM  
**Deleted:** largest

65 BC source regions, East Asia and South Asia, at present and likely in the future (e.g., Bond et al.,  
66 2007; Ohara et al., 2007; Xu et al., 2009; Lamarque et al., 2010; Menon et al., 2010).

67 The HTP, often referred to as the Third Pole, has received much less scientific attention  
68 than the Polar Regions (Qiu, 2008), although it is the highest and largest plateau that stores one  
69 of the largest ice masses of the Earth system. The HTP also has a large area of seasonal and  
70 permanent snow cover and represents the most sensitive and visible indicator of climate change  
71 with its unique location for complex interactions among the atmosphere, hydrosphere and  
72 cryosphere (e.g., Pu et al., 2007; Xu et al., 2009; Yao et al., 2012). The glaciers and the  
73 associated snowmelt over the HTP have a great potential to modify the regional hydrology and to  
74 trigger natural hazards that impact a large portion of the population in and around the region (e.g.,  
75 Barnett et al., 2005; Singh and Bengtsson, 2004; Xu et al., 2008; Kaser et al., 2010; Immerzeel et  
76 al., 2010; Yao et al., 2012; Bolch et al., 2012). The HTP also exerts profound influences on  
77 atmospheric circulation patterns and climate through mechanical and thermal effects due to its  
78 large area, highly elevated topography and geographical location in the Earth system (Yeh et al.,  
79 1957; Manabe and Terpstra, 1974; Ye and Gao, 1979; Yanai et al., 1992; Ye and Wu, 1998; Wu  
80 et al., 2012). The HTP acts as a giant wall across the Eurasian continent that blocks cold  
81 outbreaks from high latitudes in winter and confines the winter monsoon to eastern and southern  
82 Asia, while in summer, the HTP serves as a huge heat source through the strong surface sensible  
83 heating and latent heating over central and eastern Plateau (Wu et al., 2012).

84 Under the background of global warming, the climate of the HTP is changing rapidly. For  
85 example, the surface sensible heat flux has weakened in recent decades, mainly due to global  
86 warming (Duan and Wu, 2008). Observational evidence indicated that the surface air  
87 temperatures on the HTP have increased about 1.8°C over the past 50 years (Wang et al., 2008).

Hailong Wang 4/12/2015 10:56 PM

Deleted: emission

Hailong Wang 4/5/2015 3:20 PM

Deleted: Menon et al., 2002, 2010;

Hailong Wang 4/5/2015 2:49 PM

Deleted: , called the "World Water Tower",

Hailong Wang 4/5/2015 2:48 PM

Deleted: , which

Hailong Wang 4/5/2015 2:51 PM

Deleted: its significant

Hailong Wang 4/5/2015 2:53 PM

Deleted: In the winter, t

Hailong Wang 4/5/2015 2:53 PM

Deleted: ,

Hailong Wang 4/5/2015 2:53 PM

Deleted:

Hailong Wang 4/5/2015 2:53 PM

Deleted: (Wu et al., 2012)

Hailong Wang 4/5/2015 2:53 PM

Deleted: ,

Hailong Wang 4/5/2015 2:53 PM

Deleted: I

Hailong Wang 4/5/2015 2:53 PM

Deleted: the

Hailong Wang 4/5/2015 2:53 PM

Deleted: ,

Hailong Wang 4/5/2015 2:54 PM

Deleted: , with

Hailong Wang 4/5/2015 2:55 PM

Deleted: The surface sensible heat flux over the HTP has weakened in recent decades, mainly due to global warming (Duan and Wu, 2008).

Hailong Wang 4/5/2015 3:05 PM

Deleted: s

106 | while the large area at elevations above 4000 m has warmed at 0.3°C per decade in the past three  
 107 | decades (Xu et al., 2009). A number of recent studies reported that glaciers on the HTP have  
 108 | undergone widespread losses at an increasing rate in past decades (e.g., Qin et al., 2006; Li et al.,  
 109 | 2008; Kang et al., 2010; Bolch et al., 2012) and have undergone accelerated retreat in recent  
 110 | years (Yao et al., 2007). The rapid warming and the accelerated glacier retreat have been  
 111 | primarily attributed to increasing greenhouse gases (e.g., Duan et al., 2006; Ren et al., 2006), but  
 112 | other factors may be partly responsible for the accelerated warming over the HTP, such as  
 113 | atmospheric heating by absorbing aerosols, land use changes, and reduction of snow albedo  
 114 | induced by light-absorbing impurities in snow (Kang et al., 2000; Prasad and Singh 2007;  
 115 | Ramanathan et al., 2007; Flanner et al., 2007, 2009; Yasunari et al., 2010; Xu et al., 2009; Qian  
 116 | et al., 2011, 2015). Lau et al. (2006, 2010) proposed and demonstrated the Elevated Heat Pump  
 117 | mechanism, whereby heating induced by airborne BC and dust absorption can strengthen local  
 118 | circulations and lead to a northward shift of the monsoon rain belt, widespread enhanced  
 119 | warming over the HTP, and accelerated snowmelt and glacier retreat. Previous observational and  
 120 | modeling studies have indicated that BC deposition on snow and ice, which has a rapidly  
 121 | increasing trend in recent years, has been a significant contributor to the early snowmelt and  
 122 | rapid glacier retreat over the HTP (e.g., Flanner et al., 2007, 2009; Ming et al., 2008; Xu et al.,  
 123 | 2009; Kaspari et al., 2011; Menon, et al., 2010; Qian et al., 2011, 2015; Wang et al., 2015).  
 124 | Flanner et al. (2007) found that the largest regional annual mean forcing due to BC in snow is  
 125 | located in the HTP. Xu et al. (2009) and Lau et al. (2010) suggested that the BC in snow/ice may  
 126 | be partly responsible for the observed acceleration of glacier retreat in the HTP.  
 127 | Understanding the role of BC in accelerating snow-cover reduction and glacier retreat is  
 128 | becoming increasingly important. Over 60% of BC in the present-day atmosphere originates

Hailong Wang 4/5/2015 3:02 PM

Deleted: . Xu et al. (2009) reported that

Hailong Wang 4/5/2015 3:03 PM

Deleted: , which is twice the global average warming

Hailong Wang 4/5/2015 3:06 PM

Deleted: The warming trend in the cold season was greater than that in the warm season (Zhao et al., 2004).

Hailong Wang 4/5/2015 3:08 PM

Deleted: the

Hailong Wang 4/5/2015 3:09 PM

Deleted: (GHGs)

Hailong Wang 4/5/2015 3:28 PM

Deleted: Barnett et al., 2005;

Hailong Wang 4/5/2015 3:11 PM

Deleted: deposition of

Hailong Wang 4/5/2015 3:12 PM

Deleted: on

Hailong Wang 4/5/2015 3:12 PM

Deleted: (EHP)

Hailong Wang 4/5/2015 3:18 PM

Deleted: Lu et al., 2012; M.

Hailong Wang 3/31/2015 7:02 PM

Deleted: 4

Hailong Wang 4/5/2015 3:33 PM

Deleted: Qian et al. (2011) showed that the snow albedo effect of BC is more efficient in accelerating snowmelt (i.e., reducing snow cover and snow water) than warming in the atmosphere induced by greenhouse gases.

Hailong Wang 4/5/2015 3:35 PM

Deleted: Global warming, glacier retreat and snow-cover reduction have been projected to accelerate throughout the 21st century (IPCC, 2013).

Hailong Wang 4/5/2015 3:35 PM

Deleted: this

Hailong Wang 3/28/2015 12:17 AM

Deleted: A large fraction

Hailong Wang 4/14/2015 5:40 PM

Deleted: Earth system

154 from anthropogenic activities (e.g., Bond et al., 2007; Lamarque et al., 2010). Reduction of  
 155 emissions from BC-rich sources represents a potential mitigation strategy to slow down the  
 156 climate change because BC has a positive radiative forcing but a short atmospheric lifetime  
 157 (Bond et al., 2013). Since BC over the HTP may originate from a variety of geographical regions  
 158 and emission sectors, it is essential to quantify the source-receptor relationships of BC in order to  
 159 understand the contributions of open fire and anthropogenic emission sectors to BC over the  
 160 HTP. This exercise is also essential to provide guidance for potential mitigation actions.

Hailong Wang 3/28/2015 12:27 AM

**Deleted:** manage the road map of

Hailong Wang 3/28/2015 12:28 AM

**Deleted:** forcing

161 Some studies have used the conventional back-trajectory approach to identify possible  
 162 source regions for both airborne BC and that deposited on snow and ice, by tracking air mass  
 163 reaching sampling sites over the HTP (e.g., Ming et al., 2008, 2009; Cao et al., 2009; Bonasoni  
 164 et al., 2010; Zhao et al., 2013; Zhang et al., 2013). Lu et al. (2012) developed a novel back-  
 165 trajectory approach to analyze the origin of BC transported to the HTP during 1996-2010. They  
 166 derived the overall transport characteristics of BC to the HTP and showed the spatial distribution  
 167 of sources for BC reaching the HTP region based on a large set of seven-day back trajectories  
 168 arriving at the given height (i.e., 500 m) and receptor locations, BC emissions and transport  
 169 efficiencies. The statistical analysis of trajectories has good accuracy on short time scales for  
 170 source regions with close proximity to the receptor, but this approach has limitations in  
 171 determining contributions from distant sources to BC in the mid- and upper-troposphere that  
 172 could contribute significantly to the total column burden but less to BC deposition and boundary-  
 173 layer concentrations. Using the adjoint of the GEOS-Chem global chemical transport model,  
 174 Kopacz et al. (2011) attempted to identify the originating locations of BC arriving at five glacier  
 175 sites (i.e., five model grid-cells as the receptors) in the HTP for year 2001. This method can  
 176 provide a global distribution of emissions that directly contribute to BC concentrations at

Hailong Wang 4/5/2015 3:44 PM

**Deleted:** Many factors can affect the amount and impacts of BC on the HTP region, including the distance from source to the HTP, meteorological conditions that determine the transport pathways and clouds/precipitation along the pathways, and physical and chemical properties of the mixture of BC and other aerosol species that influence the interactions with clouds and subsequent wet removal during the transport.

Hailong Wang 4/4/2015 11:26 PM

**Deleted:** to also account for emissions, transformation/aging and removal processes of BC.

Hailong Wang 4/4/2015 11:26 PM

**Deleted:**

Hailong Wang 4/4/2015 11:52 PM

**Deleted:** provide the spatially and seasonally resolved source contributions to the BC atmospheric column burden above five glaciers across the HTP in 2001, using a global chemical transport model.

receptor locations. Note that the adjoint model results are not source attributions but rather the source-receptor sensitivities, which can be interpreted as the effectiveness of incremental changes to existing emissions in affecting BC at receptor locations. While the adjoint approach has the advantage of not predefining source regions, it does require performing separate simulations for each of the defined receptor regions.

In this study, we use an aerosol-climate model with a newly developed explicit source tagging approach (Wang et al., 2014) to produce a detailed characterization of the fate of BC emitted from various geographical regions and sectors (e.g., fossil fuel, biofuel and biomass burning emissions) and transport pathways to the HTP. In contrast to the back-trajectory and the adjoint approaches, the direct tagging method has the flexibility to do source attribution of BC mass mixing ratio at any model layer and the surface dry and/or wet deposition within a single simulation for any receptor regions. Section 2 describes the aerosol-climate model and the tagging method used in this study. Section 3 presents an evaluation of modeled BC surface concentrations and seasonal snow cover over the HTP region. The transport pathways and source attribution results are presented in Sect. 4. The radiative effects of BC in the atmosphere and of both BC and mineral dust in snow are compared in Sect. 5, followed by the summary and conclusions in Sect. 6.

## 2 Model Configuration and Experimental Design

### 2.1 The CAM5 model and the source-tagging method

We use the Community Atmosphere Model Version 5 (CAM5; Neale et al., 2012), which is the atmospheric component of the Community Earth System Model version 1 (CESM1) (Hurrell et al., 2013). It includes relatively comprehensive representations of aerosols and clouds, and

Hailong Wang 3/31/2015 7:02 PM

Deleted: H.

Hailong Wang 4/5/2015 12:11 AM

Deleted: s



mechanisms for their interactions with each other and with climate (Gettelman et al., 2010; Liu et al., 2012). CAM5 employs a modal aerosol module (MAM) to represent aerosols in multiple log-normally distributed modes, with internal mixing assumed for aerosol species within each individual mode, including a 3-mode standard representation (MAM3) and a more complex 7-mode representation (MAM7). The major difference between MAM3 and MAM7 related to carbonaceous aerosols lies in the treatment of aging. In MAM3, BC and primary organic matter (POM) particles are emitted into the accumulation mode that also contains highly hygroscopic species such as sulfate and sea-salt, while in MAM7 BC and POM are emitted into a primary carbon mode, which contains no other species. BC is hydrophobic upon emission, and thus the hygroscopicity of the primary-carbon-mode particles depends on the assumed hygroscopicity for POM. As more hygroscopic species (e.g.,  $\text{H}_2\text{SO}_4$  and  $\text{NH}_3$ ) condense onto the primary-carbon-mode particles, the particles are become more hygroscopic and are gradually transferred into the MAM7 accumulation mode. The rate of transfer is controlled by uncertain aging parameters, and the availability of gas precursors (Liu et al. 2012). In the accumulation mode of both MAM3 and MAM7, BC is internally mixed with other more hygroscopic species and is thus subject to wet scavenging and removal processes. During the transport from sources to remote regions, aerosols are removed too efficiently in the default CAM5 (Liu et al., 2012). Recently, H. Wang et al. (2013) revised some key processes associated with aerosol wet removal and convective transport, which significantly improved the vertical distribution of aerosols and their transport to remote regions such as the Arctic.

To better characterize the sensitivity of BC spatial distributions to emission uncertainties, Wang et al. (2014) implemented a direct source tagging method in CAM5, whereby BC emitted from a number of independent source regions and/or sectors can be tagged and explicitly tracked

Hailong Wang 3/31/2015 6:55 PM

**Deleted:**

Hailong Wang 3/31/2015 6:55 PM

**Deleted:** of the default 3-mode Modal Aerosol Module (MAM3; Aitken, accumulation and coarse modes) of CAM5

Hailong Wang 3/31/2015 6:56 PM

**Deleted:** immediately after being emitted

Hailong Wang 3/31/2015 7:02 PM

**Deleted:** H.

Hailong Wang 3/31/2015 6:58 PM

**Deleted:** the

within a single model simulation. This approach provides the quantitative characterization of source-receptor relationships for BC in any receptor region without perturbing emissions from individual BC source regions or sectors. In this study, we apply the BC tagging technique to the accumulation-mode BC in the MAM3 treatment. BC particles emitted from sixteen geographical BC source regions and two emissions sectors (i.e., biomass burning & biofuel emissions and fossil fuel emissions) in each of the regions are tagged and explicitly tracked. Instead of using the global emissions from all sectors for the original one BC mass mixing ratio variable, the thirty two regional/sectoral emissions provide sources to the respective tagged BC mass mixing ratio variables that are all added to the accumulation mode, including both interstitial and cloud-borne states. All physical and dynamic tendencies (e.g., transport, dry and wet removal) are calculated explicitly for the tagged BC mass mixing ratio variables in the same way as the original single BC mass mixing ratio. Also, when aerosol optical properties are calculated, all of the tagged BC mass mixing ratios contribute to the volume-mean refractive index of the accumulation mode that is used in the radiation calculation.

In addition to the free-running mode, CAM5 can also be configured in an offline mode, in which temperature, wind, surface fluxes (heat, moisture, and momentum), and pressure are constrained to agree closely with observations, while clouds and aerosol are allowed to evolve freely (Rasch et al., 1997; Lamarque et al., 2012; Ma et al., 2013). In this study, we run the CAM5 model in the offline mode with the direct BC source tagging capability, including the improved representation of convective transport and wet removal of aerosols. We use the NASA Modern Era Retrospective-Analysis for Research and Applications (MERRA) reanalysis dataset (Rienecker et al., 2011), using a horizontal resolution of  $1.9^{\circ} \times 2.5^{\circ}$  and 56 vertical levels. The goal is to characterize the fate of BC emitted from various geographical regions and sectors, their

transport pathways to the HTP, and their radiative forcing with seasonal variations. The simulation is performed for year 2001 with prescribed sea surface temperatures.

## 2.2 BC source regions and sectors

BC emission datasets have large uncertainties (e.g., Bond et al., 2013), and there are different inventories available for climate modeling. We use the present-day (i.e., year 2000) monthly mean emission inventories for BC provided by Lamarque et al. (2010). They were built for the climate model simulations in the Coupled Model Intercomparison Project Phase 5 (CMIP5) (Taylor et al., 2012) performed for the fifth assessment report (AR5) of the Intergovernmental Panel on Climate Change (IPCC). The AR5 BC emissions being used in our CAM5 simulation include monthly varying elevated open fire emissions (injection altitude up to 6 km), and yearly constant surface emissions from shipping and from six sectors over land: agricultural waste burning, domestic, energy, industry, transportation, and waste treatment. These surface BC emissions sectors do not distinguished between biofuel and fossil fuel combustion. To prepare for the BC source sector tagging, we divide the total surface emissions into two broader sectors, biofuel and fossil fuel, by using the ratio of biofuel to biofuel plus fossil fuel at each model grid provided by Dentener et al. (2006). We then combine the biomass burning (open fire) emissions and surface biofuel emissions, hereafter, referred to as BB (biofuel and biomass) sector. The shipping emissions are combined with the fossil fuel emissions over land to form the FF (fossil fuel) sector. Note that emissions in the BB sector have seasonal variations (associated with the open fire emissions) but the FF sector emissions used in this study have no seasonal variation at all.

The sixteen geographical BC source regions (Fig. 1a) are defined using the definition of source/receptor regions by Work Plan (WP 2.1) of the Task Force on Hemispheric Transport of

Hailong Wang 3/28/2015 12:39 AM

**Deleted:** Kopacz et al. (2011) quantified the contributions of spatially and seasonally resolved sources of BC to the atmospheric column burden above five glaciers across the HTP using the adjoint method of the GEOS-Chem (Goddard Earth Observing System-Chemistry) model for the same year 2001.

Hailong Wang 4/2/2015 11:49 PM

**Deleted:** s

304 Air Pollution (<http://iek8wikis.iek.fz-juelich.de/HTAPWiki/WP2.1>). They are ARC (Arctic),  
305 NAM (North America), CAM (Central America), SAM (South America), EUR (Europe), NAF  
306 (North Africa), SAF (South Africa), MDE (Middle East), CAS (Central Asia), SAS (South Asia),  
307 EAS (East Asia), SEA (South East Asia), PAN (Pacific, Australia and New Zealand), RBU  
308 (Russia, Belarus and Ukraine), HTP (Himalayas and Tibetan Plateau) and ROW (Rest of World).

309 Figure 1b and Table S1 in [the Supplement](#) summarize the fractional contributions of BC  
310 emissions from the different source regions and sectors. The global annual mean BC emission  
311 rate is 7.78 Tg yr<sup>-1</sup>, with 56.2% (sum of the red bars) from BB emissions (33.6% from fires and  
312 22.6% from biofuel) and 43.8% (sum of the blue bars) from FF emissions. The two largest  
313 contributors are BB emissions from SAF (about 20%) and FF emissions from EAS (about 15%),  
314 followed by BB emissions from SEA (7.7%), EAS (6.4%), SAS (6.2%) and SAM (5.7%), and  
315 EUR FF (6.4%) emissions. The geographical distributions of BC annual mean emission fluxes  
316 from BB and FF sectors for year 2000 are shown in Fig. S1 (in Supplement). [The global annual](#)  
317 [and seasonal mean lifetime of BC emitted from the tagged source regions and sectors are](#)  
318 [summarized in Table S2. On the globe average, BB BC has a longer lifetime than FF BC in all](#)  
319 [seasons, especially in boreal winter \(6.9 vs. 3.1 day\), due in part to higher open-fire emissions \(in](#)  
320 [the BB sector\) during local dry seasons. Another reason is that open-fire emissions have initial](#)  
321 [injection heights of up to 6 km, resulting in less removal below 6 km. The availability of co-](#)  
322 [emitted hygroscopic species that are internally mixed with BC in the accumulation mode of the](#)  
323 [MAM3 aerosol treatment also impacts the scavenging and wet removal rate of BC. This also in](#)  
324 [part explains the variability of BC lifetime among the different source regions and sectors.](#)  
325 [Regarding the seasonal cycle, BC emitted from the major source regions \(e.g., SAF, EAS, SEA,](#)

Hailong Wang 4/4/2015 12:31 AM

Deleted: ary Material

Hailong Wang 4/4/2015 12:33 AM

Deleted: ary Material

SAS) has substantially lower lifetime in summer (JJA) than in the other seasons, likely due to relatively strong removal by the summer monsoon precipitation.

We use two metrics for quantifying source-receptor relationships and the sensitivity of BC in a receptor region to various sources following Wang et al. (2014), but we extend them to treat BB and FF sectors separately.

1) The fractional contribution of BB and FF emissions from source region  $i$  to a BC property in the receptor region (HTP),  $C_i^{BB}$  or  $C_i^{FF}$ , is defined as

$$C_i^{BB} = \frac{A_i^{BB}}{\sum_{l=1}^N (A_l^{BB} + A_l^{FF})}, C_i^{FF} = \frac{A_i^{FF}}{\sum_{l=1}^N (A_l^{BB} + A_l^{FF})} \quad (1)$$

Where  $A_i^{BB}$  and  $A_i^{FF}$  are a BC property (e.g., mass mixing ratio, column burden, or deposition flux) in/over the receptor region resulting from BB and FF emissions, respectively, in source region  $i$ . The summation  $\sum_{l=1}^N (A_l^{BB} + A_l^{FF})$  represents the total BC from all source regions ( $N = 16$  in this study) and sectors (BB and FF). Note that for BC properties such as column burden, surface mixing ratio, and deposition flux, the tagging method in CAM5 explicitly calculates how much is due to emissions from each source region and sector.

2) Efficiency of BB and FF emissions from source region  $i$  in changing BC in a receptor region is defined as

$$S_i^{BB} = \frac{C_i^{BB}}{\left[ \frac{E_i^{BB}}{\sum_{l=1}^N (E_l^{BB} + E_l^{FF})} \right]}, S_i^{FF} = \frac{C_i^{FF}}{\left[ \frac{E_i^{FF}}{\sum_{l=1}^N (E_l^{BB} + E_l^{FF})} \right]} \quad (2)$$

Where  $C_i^{BB}$  and  $C_i^{FF}$  are the fractional contribution defined in Eq. (1), and  $E_i^{BB}$  and  $E_i^{FF}$  are the total BB and FF emission rates, respectively, in source region  $i$ . The summation  $\sum_{l=1}^N (E_l^{BB} + E_l^{FF})$  in Eq. (2) represents the global total emission rate. The efficiency metric  $S_i^{BB}$  or  $S_i^{FF}$  also characterizes the sensitivity of aerosol properties in the receptor region to per unit (BB or FF)

Hailong Wang 3/31/2015 7:02 PM  
Deleted: H.

Hailong Wang 3/23/2015 12:41 AM  
Deleted:

Hailong Wang 3/23/2015 12:42 AM  
Deleted:

emissions in the source region. This metric is of more interest to policy makers for the purpose of mitigation action, which is not the focus of this study but is worth mentioning.

### 3 Model evaluation against available observations

The CAM5 model has been evaluated in detail from different perspectives with available observations such as aerosol mass concentration, aerosol number concentration and size distribution, aerosol optical properties, cloud properties, aerosol deposition and BC in snow over various regions in previous studies (Liu et al., 2012; H. Wang et al., 2013; Ma et al., 2013; Jiao et al., 2014; Lee et al., 2013; Qian et al., 2014). Because of the complex topography and meteorology of the HTP and the relatively coarse resolution of global model, further model evaluation focusing on the HTP region is critical. Here we use near-surface atmospheric BC concentrations measured at a few HTP sites and the snow cover fraction retrieved from satellite to evaluate the CAM5 performance in the HTP.

#### 3.1 Atmospheric BC surface concentration

There are seven remote sites that have surface measurements of seasonal BC aerosol concentrations available. The locations and elevations of the sites and the sampling time periods and observation methods are described in Table 1. Figure 2 shows the comparison of seasonal mean BC concentrations between observations and CAM5 results. Note that model results represent mean concentrations in the grid box that the sampling sites reside in and at the grid-mean elevation, which could deviate significantly from the sampling point near complex terrain. All sites have non-negligible amounts of BC in the near-surface air. The error bars indicate the intra-seasonal and inter-annual variations if multi-year data were used for given season and site. However, the uncertainties of observed BC surface concentrations mainly originate from the

large discrepancies between different measurement methods, the mixing of BC with other components (e.g., organic carbon and mineral dust) in the aerosol samples, and the sampling time and location (Bond et al., 2013; Petzold et al., 2013). BC surface concentrations over the various sites show strong seasonal variations, which are reasonably captured by the model. The modeled magnitude of BC concentrations has a good agreement with observations at some sites (e.g., Fig. 2b, d, g), but the model clearly overestimates BC at the Muztagh Ata site (Fig. 2a) and underestimates at the Lulang site (Fig. 2e). The large underestimation (about 1000 m; see Table 1) of the Muztagh Ata site elevation in the model, determined by the model grid resolution, could largely explain the overestimation of BC since BC concentrations have sharp decreases with height in this region. At the sites over southern HTP (i.e., Hanle, Manora Peak, NCO-P, Lulang and NCOS), the BC surface concentrations in the summer (JJA) are lower, mainly due to wet scavenging by more frequent precipitation and partly due to the minimal emissions from domestic heating and wildfires over Himalaya foothills and Indo-Gangetic Plains (IGP) during the Indian summer monsoon season (Marinoni et al., 2010, 2013). Among all these sites, the largest BC surface concentrations occur at the Manora Peak site that is closer to the major sources in South Asia, especially in the winter (DJF) when the model underestimates the concentrations by about 50%. The high concentrations in winter at Manora Peak is mainly due to the dry winter monsoon conditions and increased transport of emissions from regional biomass burning, agricultural waste and wood fuel burning from the IGP (e.g., Ram et al., 2010; Moorthy et al., 2013). The BC surface concentrations peak in the springtime (MAM) at Hanle, NCO-P, Lulang and NCOS sites. This might be related to an increase in BB and/or FF emissions in the Indian Subcontinent, along with the higher regional boundary-layer top over the IGP during the springtime that may favor the transport of particles from the surface up to higher altitudes (e.g.,

398 Marinoni et al., 2010, 2013). Moreover, a long-range transport of pollution emitted from distant  
399 regions like the Middle East, North Africa or Europe (Marinoni et al., 2010) could further  
400 contribute to BC variability over the South Himalayas, which will also be examined in this study.  
401 Part of the discrepancies between observations and model results can be attributed to the inherent  
402 difficulty in simulating the cloud/precipitation fields over the complex topography and  
403 subsequent wet removal of aerosols during the transport, but emission uncertainties (e.g., Bond  
404 et al., 2013) might play a primary role.

### 405 3.2 Snow cover fraction

406 It is important to evaluate the performance of model in simulating seasonal snow over this region  
407 in order to assess the importance of BC-in-snow effect. Figure 3 shows the CAM5 simulated  
408 seasonal and annual mean snow cover fraction (SCF) during year 2001, in comparison to  
409 observed mean SCF, derived from the Moderate Resolution Imaging Spectrometer (MODIS)  
410 (Hall et al., 2006) monthly mean of daily products at 0.05 degree resolution. For a better  
411 comparison, the MODIS monthly mean SCFs are mapped to the CAM5 grid. The summer (JJA)  
412 season only includes July and August for both CAM5 and MODIS due to missing MODIS data  
413 in June 2001. To illustrate whether year 2001 can represent the average condition in terms of  
414 SCF, the MODIS SCF climatology (2000-2013) is also plotted. The overall SCF in HTP has very  
415 small difference between climatology and year 2001 in all seasons except for JJA, when SCF is  
416 notably higher over northwest Plateau for the climatology that included June SCF in the average.  
417 On average, SCF is about 5% (absolute amount) higher in June than in July and August. Over the  
418 52 HTP grid cells, the CAM5 SCF is highly correlated spatially with that of MODIS (for both  
419 2001 and 2000-2013) with the statistical confidence level greater than 99%, except for summer  
420 (JJA) when the linear correlation is significant only at 80% level.

Hailong Wang 4/14/2015 5:46 PM

Deleted: ,

Hailong Wang 4/14/2015 5:46 PM

Deleted: which is

Hailong Wang 4/14/2015 5:47 PM

Deleted: same grids as in the

Hailong Wang 4/14/2015 5:47 PM

Deleted: simulation



425 There are strong spatial and seasonal variations in SCF due to the complex terrain and  
426 seasonal variation in snowfall and melting. The SCF over the entire HTP reaches the maximum  
427 in the winter (DJF), while decreases to almost none (less than 5%) in July and August. Snow  
428 covers the western and southeastern Plateau during the transition seasons (MAM and SON). The  
429 CAM5 simulation shows a good agreement with MODIS in the annual mean (ANN) SCF and the  
430 strong seasonality. The most persistent snow cover at the southern and western edges of the HTP  
431 and the relatively less persistent in the HTP interior are captured by the CAM5 model. The  
432 performance of the CAM5 has been improved, in comparison to its earlier version (CAM3) that  
433 remarkably overestimated the SCF especially over the HTP interior (Qian et al., 2011), although  
434 the CAM5 still significantly overestimates the SCF in the western Plateau in DJF and MAM and  
435 underestimates it in JJA. The CAM3 model used by Qian et al. (2011) overestimates SCF by up  
436 to a factor of 2 during the cold season (November to April). The CAM3 spring (MAM) mean  
437 SCF is greater than 35%, while the CAM5 spring mean (21%) in the present study is in good  
438 agreement with the MODIS spring SCF (18±5%).

Hailong Wang 3/31/2015 5:01 PM

Deleted: dramatically

439 Although we believe that the CAM5 SCF biases are qualitatively robust, it is worth  
440 noting that the MODIS products have uncertainties as well. Pu et al. (2007) evaluated the  
441 MODIS SCF products over the HTP against ground-based snow observations and showed that  
442 total error in MODIS SCF products over the HTP is about 10%. However, their analysis based  
443 on MODIS eight-day snow-cover composite gave a significantly higher SCF (more than 10%)  
444 than the one we show here using daily products, especially, in winter and early spring.  
445 Interestingly, based on a different source of observation, Qin et al. (2006) found that snow covers  
446 about 59% of the Tibetan Plateau in winter, which is comparable to the mean SCF (50%) in our

Hailong Wang 3/29/2015 12:27 AM

Deleted: very close

CAM5 simulation. Nonetheless, we keep this discrepancy in mind when interpreting the wintertime BC-in-snow radiative forcing that suffers the most from such potential SCF bias.

## **4 Modeled transport pathways and source attribution of BC in the HTP**

### **4.1 Transport pathways**

The direct source tagging method can clearly characterize the three-dimensional transport pathways of BC emitted from various source regions and sectors to the HTP receptor region. General circulation patterns over the HTP and surroundings are typically affected by mid-latitude westerlies in the winter and Asian monsoon in the summer, including the South Asian summer monsoon and East Asian summer monsoon (Xu et al., 2009; Yao et al., 2012; Wu et al., 2012; also see Fig. S2).

Figure 4 illustrates circulation patterns over HTP and BC transport pathways from six major source regions to the HTP in the winter (DJF) and summer (JJA). (See similar plots in Figs. S3–S5 for other tagged source regions.) In the winter, the strong surface cooling over the HTP leads to subsidence/divergence and the formation of an enhanced local circulation cell, while in the summer air converges toward the HTP from the surroundings, particularly from the South Asia, due to the ascending of strongly heated air over the HTP (e.g., Wu et al., 2012), as also indicated by the arrows in the vertical cross-sections in Fig. 4. In the winter, the subtropical westerlies extend to about 10°N in mid-/upper troposphere and 20°N near surface, and the tropical easterlies are weak (see the white contours of latitude-height cross-section panels in Fig. 4). The circulation patterns near the HTP change dramatically during the summer monsoon season. The reversal of surface wind regime in the tropics (e.g., Arabian Sea, Bay of Bengal, and

471 South China Sea) is characteristic of the Asian summer monsoon climate (see Fig. S2e, g). The  
472 subtropical westerlies recede to north of 30°N and the center of the westerly jet shifts to about  
473 40°N in JJA (from about 30°N in DJF). The strong easterlies characterize the upper troposphere  
474 of tropical region (south of HTP), while the southwesterly flow prevails in the lower troposphere  
475 (white contours of latitude-height cross-section panels in Fig. 4). The prevailing winds during the  
476 transition seasons (MAM and SON) between DJF and JJA are still westerlies (Fig. S2b, d).

477 The circulation patterns determine the transport of BC around the HTP region. However,  
478 the variations of spatial distributions of BC emitted from the different source regions and in  
479 different seasons could be due to the differences in source location and strength, wet removal  
480 rate and lifting. Note that although we combined BC emitted from BB and FF sections to  
481 characterize transport pathways in Fig. 4, only BC emissions from BB sector have seasonal  
482 variations in the emission inventory we use.

483 The HTP region is surrounded by two major BC source regions, SAS and EAS (Fig. 1a),  
484 which potentially have great impact on BC in the HTP (e.g., Menon et al., 2010; Bond et al.,  
485 2007; Ohara et al., 2007; Xu et al., 2009; Kopacz et al., 2011; Lu et al., 2012). BC emissions  
486 from SAS are dominated by the BB sector, and by FF sector from EAS (Fig. 1b). As shown in  
487 Fig. 4, in the winter, a significant amount of BC from SAS can be transported to the eastern  
488 Plateau by the strong westerlies under the dry winter monsoon conditions. During the South  
489 Asian summer monsoon BC from SAS is effectively removed by the local abundant  
490 precipitation, as indicated by the low lifetime in summer (Table S2), but can still affect large area  
491 in the southwest of the HTP. However, BC from EAS can be uplifted higher and transported  
492 more to the Northeast Plateau in the summer monsoon season than in the winter. Along the  
493 wintertime westerlies, BC from upwind source regions (e.g., EUR, NAF, SAF, MDE, and CAS)

Hailong Wang 4/5/2015 3:19 PM

Deleted: 2002,

Hailong Wang 4/4/2015 11:21 PM

Deleted: a

Hailong Wang 3/29/2015 1:36 AM

Deleted: I

497 can easily move to the HTP, while the HTP local emissions are transported far away (Fig. 4). BC  
498 originating from the distant sources such as SAF and MDE reaches up high (to 300hPa) in the  
499 HTP. In the summer, continental deep convection can loft BC into higher altitudes where it can  
500 be transported to the HTP along the relatively weaker westerlies from upwind source regions  
501 (e.g., EUR, RBU, MDE, and CAS). However, BC from distant low-latitude source regions such  
502 as SAF barely reaches the HTP region due to weak emissions but strong removal along the  
503 transport pathways to the HTP during the summer monsoon season.

#### 504 4.2 Seasonal variation of BC in the HTP

505 BC concentrations in the HTP have strong dependence on season and location. Figure 5 shows  
506 the annual mean and seasonal variations of BC column burden and deposition rate over the HTP  
507 and five sub-regions. The seasonal variation of the ratio of wet to total BC deposition is  
508 superimposed. The Central Plateau is the cleanest region during all seasons, compared to other  
509 sub-regions in the HTP (Fig. 5e). Both BC column burden and deposition rate from the BB  
510 sector peak in MAM over the HTP, mostly in the Himalayas and Southeast Plateau region. The  
511 FF BC burden in the HTP peaks in the summer mainly due to the seasonal maximum over  
512 Northwest and Northeast Plateaus. However, BC wet removal rate over the Northwest Plateau is  
513 at minimum in the summer, as opposed to the summer maximum in other sub-regions and the  
514 entire HTP region. For Himalayas, Southeast and Central Plateau, the seasonal variation (i.e.,  
515 maximum in MAM followed by a sharp decrease to JJA) of BB and FF column burden (Fig. 5c,  
516 d and e) is similar to the variation of observed surface concentrations at sites located in these  
517 sub-regions (Fig. 2b, d, e and f). In the Himalayas and Southeast Plateau, the ratio of regional  
518 mean BC column burden to deposition rate (Fig. 5c and d), indicator of removal time scale or  
519 lifetime, is the smallest (less than 1 day) during the Asian summer monsoon (JJA) due to the

Hailong Wang 4/14/2015 6:00 PM

Deleted: s

Hailong Wang 4/14/2015 6:00 PM

Deleted: s

522 efficient wet scavenging of BC by abundant precipitation. In Northwest and Northeast Plateau,  
523 the BC column burden increases from DJF to JJA and reaches the maximum in JJA, and then  
524 decreases in SON (Fig. 5b and f), partly due to the peak contribution of EAS and CAS emissions  
525 in JJA. This trend is also similar to that in the observed surface concentrations (Fig. 2a and g).  
526 The deposition rate follows the same seasonal variation of column burden over the Northeast  
527 Plateau, while the deposition has a minimum in JJA over the Northwest Plateau when the column  
528 burden is at maximum likely due to the less efficient wet removal in this region (Fig. 5b and f).

529 The annual mean BC column burden over the HTP has almost the same contributions  
530 from BB and FF emission origins, with BB dominating in DJF and MAM and FF in JJA. In the  
531 Himalayas, BC is predominantly from BB sector for all seasons (Fig. 5c). In the Southeast and  
532 Central Plateaus, the dominant source sector is BB in DJF and MAM, but FF dominates in JJA.  
533 The dominant source sector over the Northwest and Northeast Plateaus is always FF, especially  
534 in the summer. We need to analyze the source-receptor relationships in order to quantify the  
535 roles of BB and FF emissions from the various source regions in determining BC over the HTP  
536 and the sub-regions.

### 537 4.3 BC source-receptor relationships

538 Previous studies (e.g., Xu et al., 2009; Kopacz et al., 2011) have shown that BC and its source-  
539 receptor relationships vary significantly with season and location in the HTP. We intend to  
540 quantify source contributions to BC at different locations of the HTP and in different seasons.  
541 Our analysis also shows that the relative contributions to BC from different source regions and  
542 sectors depend on season and location in the HTP. As shown in Fig. 6, the largest contribution to  
543 the annual mean BC burden and surface deposition for the entire HTP region is from BB

Hailong Wang 4/5/2015 5:42 PM

Deleted: s

Hailong Wang 4/5/2015 5:42 PM

Deleted: the

Hailong Wang 4/5/2015 5:42 PM

Deleted: s

emissions from SAS, followed by FF emissions from SAS and then the FF from EAS. The same roles hold for all the seasonal means except for the summer (JJA) when the EAS FF becomes more important for BC column burden in the HTP and, to a lesser extent, for deposition.

The SAS emissions account for 50% of the annual mean burden over the HTP, including 33% from BB and 17% from FF. The other 50% is mostly from the EAS (5% BB and 14% FF), HTP (6% BB and 6% FF), CAS FF (4%), MDE FF (4%) and SAF BB (3%). The source attribution for annual mean BC deposition for the entire HTP is similar, but SAS contributes even more to BC deposition than to the column burden. Although RBU has a lower contribution to the annual mean BC in the HTP than the six regions shown in Fig. 6, its contribution to the JJA mean, especially at some locations, is quite substantial (included in the black bar) and even more important than some of the six regions in Fig. 6, as discussed in detail below.

BC annual mean burden over the HTP has nearly equal contributions from BB and FF emissions. However, contribution by BB emissions, mainly from SAS, is larger than from FF sector in DJF and MAM. In the summer (JJA), the largest contribution (about 29%) to HTP BC is from EAS FF emissions. This is partly due to the change of circulation patterns (Fig. 4) and effective wet removal of SAS BB emissions. Note that EAS FF emissions are much larger than FF emissions from any other of the source regions, and are more than twice the EAS BB emissions.

For BC in the five finer receptor regions of interest (as defined in Fig. 5g), SAS BB and FF have the largest contribution to BC in Himalayas and Central Plateau, while EAS FF and BB contribute the most to Northeast Plateau in all seasons and Southeast Plateau in the summer.

568 Central Asia and Middle East FF emissions have relatively more important contribution to BC  
569 reaching Northwest Plateau, especially in the summer.

570 For the Northwest Plateau (Fig. 6b), the prevailing winds in this sub-region are westerly  
571 throughout the year (Fig. S2; Cao et al., 2009; Xu et al., 2009), so the important source regions  
572 ought to locate at the west of HTP (e.g., MDE, EUR, and parts of SAS and RBU in Fig. 1a). SAS  
573 emissions are still the dominant source for the annual BC burden in this sub-region (17% from  
574 BB and 14% from FF), followed by HTP local emissions (9% from BB and 13% from FF), CAS  
575 (2% from BB and 14% from FF), MDE FF (8%) and EAS FF (7%). BC emissions from SAS are  
576 the dominant source in DJF, MAM and SON. CAS becomes the dominant source region (5%  
577 from BB and 26% from FF) in JJA, even though CAS is not a significant emission source region  
578 on a global basis (Fig. 1b). BC emitted from MDE is predominantly in the FF sector throughout  
579 the year. Emissions from the rest of the tagged sources (in addition to the top six) become more  
580 significant in this sub-region (black color in Fig. 6b), mostly from EUR and RBU through long-  
581 range transport (Fig. S3). The source attribution for BC deposition in this sub-region is similar to  
582 that of the column burden, but BC emitted from SAS and MDE appears to be more efficient in  
583 deposition except for the JJA season when BC from EAS contributes more to deposition than to  
584 column burden.

585 The Himalayas sub-region located along the southern edge of the HTP is in close  
586 proximity to the SAS. Thus emissions from SAS are absolutely the dominant source for BC in  
587 Himalayas throughout the year. This sub-region receives more BC from BB sector than FF  
588 because BC emissions in SAS are mainly in the BB sector, especially in MAM season (Fig. 1b  
589 and Fig. S6). For the annual mean burden, BC from SAS contributes 81% (54% from BB and  
590 27% from FF), followed by HTP local emissions (6% from BB and 3% from FF). It is worth

591 noting that SAF BB emissions contribute about 10% to burden in DJF through a long-range  
592 transport. BC deposition in this sub-region also predominantly originates from SAS, which is  
593 consistent with previous studies by Ming et al. (2008) and Kopacz et al. (2011).

594 For the Southeast Plateau (Fig. 6d), the BC source contribution profile is similar to that of  
595 Himalayas during DJF and MAM season, in which SAS is still the dominant source, especially  
596 in MAM (74% contribution to column burden, including 53% from BB and 21% from FF),  
597 although the contribution from EAS is larger here than for the Himalayas. As also pointed by  
598 Ramanathan et al. (2007), BC over the SAS can be transported to the Southeast Plateau by the  
599 southern branch of the westerlies during the winter and spring. However, the BC source  
600 contribution profile changes dramatically during the summer when emissions in EAS become the  
601 dominant source to this sub-region (68% to column burden, including 23% from BB and 45%  
602 from FF). Kopacz et al. (2011) also found that the BC from south-eastern China is the dominant  
603 contributor to the Southeast Plateau in July. For the annual mean burden in this sub-region, SAS  
604 is still the dominant contributor (40% from BB and 17% from FF), followed by EAS (8% from  
605 BB and 15% from FF), HTP (6% from BB and 6% from FF). BC originating from EAS  
606 contributes more to deposition than to burden in this sub-region.

607 For the Central Plateau (Fig. 6e), source attribution profiles for annual and seasonal BC  
608 are very similar to those of the entire HTP region with SAS being the dominant source region  
609 throughout the year except that EAS has comparable contributions in JJA. Ming et al. (2010)  
610 pointed out that pollutants from the Indo-Gangetic Basin could be transported to the Central  
611 Plateau by both the summer monsoon and the westerlies. Xia et al. (2011) also found that the  
612 substantial regional atmospheric brown haze from the nearby regions of SAS is the main source



613 for the background aerosols in the Central Plateau based on sunphotometer and satellite  
614 observations.

615 Compared to the other sub-regions, the Northeast Plateau receives the largest contribution  
616 of BC from EAS throughout the year (50% to annual mean burden, including 12% from BB and  
617 38% from FF; see Fig. 6f), especially in JJA (17% from BB and 49% from FF). The EAS FF  
618 sector contribution and the magnitude of burden (Fig. 5f) over the Northeast Plateau have strong  
619 seasonal variations, mostly due to variations in meteorology because the FF emissions in our  
620 simulation do not vary seasonally. Kopacz et al. (2011) indicate that the primary contribution to  
621 BC over the Northeast Plateau is from western China during January and April (transported by  
622 mid-tropospheric westerlies), and from central-eastern China during July and October  
623 (transported by boundary layer flow). Other main contributions to BC burden over the Northeast  
624 Plateau include 13% from SAS and 10% from HTP local emissions. Similar to the Northwest  
625 Plateau, some other upwind source regions (e.g., CAS, MDE, RBU and EUR) have a significant  
626 contribution to the Northeast sub-region as well.

#### 627 4.4 Seasonal variation of HTP BC sensitivity

628 Following Wang et al. (2014), we defined the “efficiency” metric in Sect. 2.2 to quantify the  
629 sensitivity of BC response to absolute change (e.g., per unit perturbation) of emissions in  
630 different source regions. This metric has the value of 1 if the entire globe is treated as a single  
631 source region, so we may assume the global mean efficiency of 1 as a reference to measure the  
632 sensitivity to perturbation from different source regions/sectors.

633 Figure 7 shows efficiencies of tagged sources in affecting the BC seasonal and annual  
634 mean column burden and deposition in the HTP and five sub-regions (as defined in Fig. 5g). BC

Hailong Wang 3/31/2015 7:03 PM

Deleted: H.

Hailong Wang 4/5/2015 5:03 PM

Deleted: relative

in the same receptor regions is generally most sensitive to change in local emissions, regardless of seasons, emission sectors and locations of receptor regions. Among all the source regions, although the HTP local (FF+BB) emissions only contribute about 10%, BC in the HTP is extremely sensitive to changes in the emissions within HTP. In addition to the local emissions, BC in the HTP is also sensitive to emissions in neighboring source regions (e.g., SAS and CAS) and emissions from distant sources such as MDE. Not only does the SAS have large contribution to BC burden and deposition over the HTP, as well as most of the sub-regions except for the Northeast Plateau (receptor V), but also the efficiencies for SAS emissions are high for almost all of the sub-regions especially the Himalayas (receptor II). BC in the Northeast Plateau (receptor V) is quite sensitive to EAS emissions in all seasons, while BC in the Southeast Plateau is sensitive to EAS emissions in JJA and SON. Although BC emissions from MDE and CAS are weak (Fig. 1b) and their contributions to the HTP are relatively low, their efficiencies are high. BC over Northwest Plateau (receptor I) and Central Plateau (receptor IV) is extremely sensitive to emissions from CAS in JJA. These source-receptor relationships of sensitivity will provide useful information for policymakers to improve the effective mitigation road map in order to potentially slow down the glacier retreat in the HTP region.

## **5 Radiative forcing**

The BC-in-snow effect can be quantified using the online calculation of radiative forcing in the SNICAR (Snow, Ice, and Aerosol Radiative) model (Flanner et al., 2007) coupled to CAM5, and then compared to airborne BC radiative forcing. Figure 8 shows seasonal and annual mean BC all-sky shortwave direct radiative forcing (DRF) at the surface (dimming) and the top of the

659 atmosphere (TOA), and the BC-in-snow radiative forcing (darkening) averaged over the entire  
 660 HTP and the five sub-regions (as defined in Fig. 5g). Note that the BC-in-snow forcing is  
 661 averaged over all model grids in the area (i.e., zero enters the calculation for any grid when snow  
 662 is not present). The radiative forcing of BC (and dust) in snow is small in JJA and SON due to a  
 663 lack of snow cover (Fig. 3). The forcing maximum occurs during the spring melt (MAM) when  
 664 the insolation is rather intense and BC accumulates at the surface of the snowpack as the snow  
 665 melts (Conway et al., 1996; Flanner et al., 2007, 2009), and when the snow-albedo feedback is  
 666 strongest (Hall and Qu, 2006). This strong seasonal variation also explains why the coefficient of  
 667 variation (i.e., the ratio of the SD to the mean) is greater than 1 for the annual mean BC-in-snow  
 668 forcing over the entire HTP and all sub-regions. The seasonal variations of airborne BC DRF at  
 669 the TOA and surface are consistent with that of the BC column burden (Fig. 5). For the entire  
 670 HTP (Fig. 8a1), the annual mean surface radiative forcing due to BC in snow ( $0.42 \text{ W m}^{-2}$ )  
 671 exceeds the BC dimming effect at the surface ( $-0.3 \text{ W m}^{-2}$ ). The annual mean BC-in-snow  
 672 forcing is even higher over the Northwest Plateau (Fig. 8b1) and Himalayas (Fig. 8c1), and far  
 673 exceeds the other forcings in the same sub-regions, although the BC-in-snow effect may be  
 674 overestimated due to the potential positive bias in snow cover fraction in our simulation (Fig. 3).  
 675 The annual mean BC surface dimming exceeds the BC-in-snow effect in the Southeast (Fig. 8d1),  
 676 Central (Fig. 8e1) and Northeast Plateau (Fig. 8f1). The minima of all BC-related forcings  
 677 appear in the Central Plateau where the BC burden and deposition are the lowest among all the  
 678 sub-regions (Fig. 5), and the SCF is very small (Fig. 3).

679 We have also calculated an approximate source attribution for the BC-in-snow radiative  
 680 forcing over the HTP and its sub-regions, using the tagged-source BC deposition, which is  
 681 simply assumed to be linearly proportional to BC-in-snow radiative forcing. The SCF is taken

682 into account in the calculation (i.e., the deposition at each model grid is multiplied by SCF when  
683 calculating the area-average deposition). Overall, despite small quantitative differences, the  
684 source contributions to BC-in-snow forcing are similar to those for BC deposition (Fig. 6). The  
685 SAS BB emissions contribute the most to annual mean forcing over the HTP and sub-regions  
686 except for the Northeast Plateau that is mostly contributed by EAS FF emissions. During the  
687 winter and spring seasons over Northwest Plateau and Himalayas, when and where the forcing is  
688 the largest, SAS (especially the BB sector) is the major contributor.

689 Dust is a major contributor to the total aerosol burden over the HTP (e.g., Zhang et al.,  
690 2001). Although we don't focus on other snow impurities such as mineral dust, it is worth noting  
691 that dust-in-snow radiative forcing has been considered in our model simulation and it could be  
692 an important forcing agent. We also plotted dust-in-snow forcing over the HTP and sub-regions  
693 in Fig. 8 (along with the BC-induced forcings). The annual mean dust-in-snow forcing ( $0.33 \text{ W m}^{-2}$ )  
694 is comparable to all of the other forcings over the HTP, especially in the springtime when  
695 dust outbreaks and can be transported to the HTP from the surrounding sources such as  
696 Taklimakan and Gobi deserts (Liu et al., 2008). The annual mean dust-in-snow forcing is as large  
697 as  $0.99$  and  $0.59 \text{ W m}^{-2}$  in the Northwest and Northeast Plateau, respectively (Fig. 8b1 and f1),  
698 which is in close proximity to the Taklimakan Desert (Huang et al., 2007; Chen et al., 2013), but  
699 negligibly small in the Southeast Plateau and Central Plateau. In the winter, the dominant dust in  
700 snow effect over Northeast Plateau is consistent with the recent observations. Huang et al. (2011),  
701 X. Wang et al. (2013) and Zhang et al. (2013) found that insoluble light-absorbing particles in  
702 snow are dominated by local soil and desert dust in the Qilian Mountain (Northeast Plateau).

703 Both snow cover fraction (SCF) and mass concentration of snow impurities affect the  
704 calculation of radiative forcing in snow. We have evaluated the model estimation of SCF in

different seasons (Fig. 3). We have also compared BC concentration and deposition flux from our model results to a recent modeling study by Ménéguez et al. (2014) and to observations in the HTP (Ginot et al., 2014) (Table S3). Bond et al. (2013) pointed out that observations of BC in snow pits or ice cores mostly involve snow/ice samples obtained in the summer and early fall, when almost all grid boxes the sample sites located in are snow free in the HTP. They also indicated that the CAM3 global climate model (Flanner et al., 2009) may be overestimating snow BC concentrations in the HTP, especially in the spring. Our comparison shows that despite a smaller bias than in Ménéguez et al. (2014) the CAM5 model still largely overestimates BC concentrations in snow but underestimates dust concentrations in snow over the HTP. Ménéguez et al. (2014) provided a few possible reasons for the differences between model simulations and observations. Factors such as measurement uncertainties (due to sample treatment and analysis methodology), temporal (inter-annual and seasonal) and spatial variations of BC deposition, and vertical variations of BC in snowpack, can strongly affect the accuracy and representativeness of BC-in-snow measurements for the purpose of evaluating global models. Ming et al. (2013) and Qian et al. (2015) pointed out that BC concentrations in snow and ice samples over HTP tend to decrease with increasing glacier elevations, while global models with coarse grid resolution cannot accurately represent elevation of sampling sites. Often times the difference is significant. Nonetheless, it is likely that positive biases exist in the modeled concentration and radiative forcing of BC and dust in snow.

## 6 Summary and conclusions

In this study, we employed the CAM5 model with a newly developed source tagging technique, nudged towards the MERRA meteorological reanalysis, to characterize the fate of BC particles emitted from various geographical regions and sectors to the HTP region. In addition, we

Hailong Wang 4/2/2015 11:31 PM

Deleted: 2

compare the radiative forcing induced by BC in the atmosphere and in snow over the HTP, as well as forcing induced by dust in snow. Although there are biases in the simulated BC, partly due to the inherent difficulty for coarse-resolution global models to accurately represent transport and wet deposition in this topographically complex region, the CAM5 model simulation shows a reasonable agreement in the seasonal variation of the near-surface airborne BC concentrations with observations over the HTP and surrounding regions. This provides us the confidence to use this modeling framework to characterize BC source-receptor relationships in the HTP. Using very different approaches, Kopacz et al. (2011), Lu et al. (2012) and the present study all show that South Asia and East Asia are the main source regions for BC transported to the HTP, while the magnitude of contributions from each of the source regions varies with season and receptor location. Although all of the three studies can provide quantitative source attributions, a quantitative inter-comparison of the findings is quite difficult, given the differences in the definition of geographical source and receptor regions, emission inventories, time periods for model simulation, and analysis methods. Nevertheless, in addition to quantifying the contributions of source regions, our direct source tagging approach allows us to further break down regional contributions by sectors (i.e., fossil fuel vs. biomass & biofuel) and to characterize the transport pathways of individual regional/sectoral emissions.

The explicit source tagging technique enables the characterization of three-dimensional transport pathways of BC to the HTP from different geographical regions and source sectors, which also depends on seasons and the location of the receptor in the HTP. With the IPCC AR5 present-day emission inventories, the annual mean BC column burden and surface deposition in the entire HTP region is contributed the most by biomass and biofuel (BB) emissions from South Asia (SAS) (33% and 40%, respectively), followed by fossil fuel (FF) emissions from SAS (17%

and 20%, respectively), and then the FF from East Asia (EAS) (14% and 14%, respectively). The same roles hold for all the seasonal means except for the summer when the EAS FF becomes more important. Although BC emissions from the entire EAS source region are much stronger than those from SAS, the concentrated FF BC emissions in central-eastern China are only transported towards the HTP during the East Asian summer monsoon. Thus seasonal prevailing winds are important in determining the seasonal variations in BC transport and source-receptor relationships.

Both the annual and seasonal mean BC properties and their source-receptor relationships vary significantly with location in the HTP. For the multiple finer receptor regions of interest, SAS BB and FF have the largest impact on BC in Himalayas and Central Plateau, while EAS FF and BB contribute the most to Northeast Plateau in all seasons and Southeast Plateau in the summer. The Central Asia (CAS) and Middle East (MDE) FF emissions make important contributions to BC over the Northwest Plateau, especially from CAS in JJA.

The HTP BC is most sensitive by far to per unit changes in the local emissions, although they only contribute about 10% to the BC burden in the HTP. The SAS region makes large contributions to BC burden and deposition over the HTP and the BC sensitivities to SAS emissions are also high for almost all of the sub-regions of HTP, especially the Himalayas. BC over the Northeast Plateau is quite sensitive to EAS emissions in all seasons, and Southeast Plateau BC is also sensitive to EAS emissions in JJA. Although BC emissions from MDE and CAS are weak and their contribution to the HTP overall is low, their efficiencies are quite high. BC over Northwest Plateau and Central Plateau is extremely sensitive to emissions from CAS in JJA. These source-receptor relationships and sensitivities can be useful to policymakers for

improving the effective mitigation road map in order to potentially slow down the glacier retreat in the HTP region.

The impact of BC on snow and glacier melting can be characterized by the magnitude of radiative forcing. Our calculations show that the annual mean BC-in-snow radiative forcing ( $0.42 \text{ W m}^{-2}$ ) outweighs BC dimming effect ( $-0.3 \text{ W m}^{-2}$ ) at the surface over the HTP. In the five sub-regions, the annual mean BC-in-snow forcing ranges from  $0.04 \text{ W m}^{-2}$  in the Central Plateau to  $1.75 \text{ W m}^{-2}$  in the Northwest Plateau. We also showed that the annual mean dust-in-snow induced radiative forcing over the HTP can be quite significant ( $0.33 \text{ W m}^{-2}$  for entire the HTP, and  $0.99 \text{ W m}^{-2}$  for the Northwest Plateau). More importantly, both BC- and dust-in-snow forcing peaks in the spring melting season when the area-average forcing reaches  $1.03$  and  $0.87 \text{ W m}^{-2}$ , respectively, over the entire HTP, and their combined forcing is more than  $8 \text{ W m}^{-2}$  over the Northwest Plateau. Such a large forcing is sufficient to cause earlier snow melting and contribute to the acceleration of glacier retreat, although the model is likely to overestimate BC-in-snow forcing due to the possible positive bias of snow cover fraction in the winter and early spring. According to our estimates of the source attribution, the biomass burning and biofuel emissions in South Asia contribute the most to annual mean forcing over the HTP and its sub-regions except for the Northeast Plateau where the largest contribution is from East Asia fossil fuel emissions. During the winter and spring seasons over Northwest Plateau and Himalayas, when and where the forcing is the largest, South Asia (especially the biomass burning and biofuel sector) is the major contributor.

*Acknowledgments.* This research is based on work supported by the U.S. Department of Energy (DOE), Office of Science, Biological and Environmental Research as part of the Earth System Modeling Program. The Pacific Northwest National Laboratory (PNNL) is operated for DOE by Battelle Memorial



800 Institute under contract DE-AC05-76RLO1830. The CESM project is supported by the National Science  
 801 Foundation and the DOE Office of Science. R. Zhang acknowledges support from the China Scholarship  
 802 Fund. J. Huang and Q. Fu acknowledge support from the National Basic Research Program of China  
 803 (2012CB955303), NSFC grant 41275070 and China 111 project (No. B13045). Computational resources  
 804 were provided by the National Energy Research Scientific Computing Center (NERSC), a national  
 805 scientific user facility located at Lawrence Berkeley National Laboratory in Berkeley, California. NERSC  
 806 is the flagship scientific computing facility for the Office of Science in DOE.

805

## 806 References

- 807 Babu, S. S., Chaubey, J. P., Moorthy, K. K., Gogoi, M. M., Kompalli, S. K., Sreekanth, V., Bagare, S. P., Bhatt, B.  
 808 C., Gaur, V. K., Prabhu, T. P., and Singh, N. S.: High altitude (~4520 m amsl) measurements of black  
 809 carbon aerosols over western trans-Himalayas: Seasonal heterogeneity and source apportionment, *J.*  
 810 *Geophys. Res.*, 116, D24201, doi:10.1029/2011JD016722, 2011.
- 811 Barnett, T. P., Adam, J. C., and Lettenmaier, D. P.: Potential impacts of a warming climate on water availability in  
 812 snow-dominated regions, *Nature*, 438, 303–309, doi:10.1038/Nature04141, 2005.
- 813 Bolch, T., Kulkarni, A., Kääb, A., Huggel, C., Paul, F., Cogley, J., Frey, H., Kargel, J., Fujita, K., Scheel, M.,  
 814 Bajracharya, S., and Stoffel, M.: The state and fate of Himalayan Glaciers, *Science*, 336, 310–314,  
 815 doi:0.1126/science.1215828, 2012.
- 816 Bond, T. C., Bhardwaj, E., Dong, R., Jogani, R., Jung, S., Roden, C., Streets, D. G., and Trautmann, N. M.:  
 817 Historical emissions of black and organic carbon aerosol from energy-related combustion, 1850–2000,  
 818 *Global Biogeochem. Cy.*, 21, GB2018, doi:10.1029/2006GB002840, 2007.
- 819 Bond, T. C., Doherty, S. J., Fahey, D. W., Forster, P. M., Berntsen, T., DeAngelo, B. J., Flanner, M. G., Ghan, S.,  
 820 Kärcher, B., Koch, D., Kinne, S., Kondo, Y., Quinn, P. K., Sarofim, M. C., Schultz, M. G., Schulz, M.,  
 821 Venkataraman, C., Zhang, H., Zhang, S., Bellouin, N., Guttikunda, S. K., Hopke, P. K., Jacobson, M. Z.,  
 822 Kaiser, J. W., Klimont, Z., Lohmann, U., Schwarz, J. P., Shindell, D., Storelvmo, T., Warren, S. G., and  
 823 Zender, C. S.: Bounding the role of black carbon in the climate system: A scientific assessment, *J. Geophys.*  
 824 *Res.-Atmos.*, 118, 5380–5552, doi:10.1002/jgrd.50171, 2013.
- 825 Bonasoni, P., Laj, P., Marinoni, A., Sprenger, M., Angelini, F., Arduini, J., Bonafé, U., Calzolari, F., Colombo, T.,  
 826 Decesari, S., DiBiagio, C., di Sarra, A. G., Evangelisti, F., Duchi, R., Facchini, MC., Fuzzi, S., Gobbi, G. P.,  
 827 Maione, M., Panday, A., Roccatò, F., Sellegri, K., Venzac, H., Verza, GP., Villani, P., Vuillermoz, E., and  
 828 Cristofanelli, P.: Atmospheric Brown Clouds in the Himalayas: first two years of continuous observations  
 829 at the Nepal Climate Observatory-Pyramid (5079 m), *Atmos. Chem. Phys.*, 10, 7515–7531,  
 830 doi:10.5194/acp-10-7515-2010, 2010.
- 831 Cao, J. J., Xu, B. Q., He, J. Q., Liu, X. Q., Han, Y. M., Wang, G. H., and Zhu, C. S.: Concentrations, seasonal  
 832 variations, and transport of carbonaceous aerosol at a remote Mountainous region in western China, *Atmos.*  
 833 *Environ.*, 43, 4444–4452, doi:10.1016/j.atmosenv.2009.06.023, 2009.

834 Chen, S., J. Huang, C. Zhao, Y. Qian, L. R. Leung, and B. Yang: Modeling the Transport and Radiative Forcing of  
835 Taklimakan Dust over the Tibetan Plateau in Summer, *J. Geophys. Res.*, 118, 797–812,  
836 doi:10.1002/jgrd.50122, 2013.

837 Conway, H., Gades, A., and Raymond, C. F.: Albedo of dirty snow during conditions of melt, *Water Resour. Res.*,  
838 32, 1713–1718, doi:10.1029/96WR00712, 1996.

839 Dentener, F., Kinne, S., Bond, T., Boucher, O., Cofala, J., Generoso, S., Ginoux, P., Gong, S., Hoelzemann, J. J., Ito,  
840 A., Marelli, L., Penner, J. E., Putaud, J.-P., Textor, C., Schulz, M., van der Werf, G. R., and Wilson, J.:  
841 Emissions of primary aerosol and precursor gases in the years 2000 and 1750 prescribed data-sets for  
842 AeroCom, *Atmos. Chem. Phys.*, 6, 4321–4344, doi:10.5194/acp-6-4321-2006, 2006.

843 Doherty, S. J., Dang, C., Hegg, D. A., Zhang, R., and Warren, S. G.: Black carbon and other light-absorbing  
844 particles in snow of central North America, *J. Geophys. Res. Atmos.*, 119, 12,807–12,831,  
845 doi:10.1002/2014JD022350, 2014.

846 Duan, A., Wu G., Zhang Q., and Liu Y.: New proofs of the recent climate warming over the Tibetan Plateau as a  
847 result of the increasing greenhouse gases emissions, *Chin. Sci. Bull.*, 51, 1396–1400, doi:10.1007/s11434-  
848 006-1396-6, 2006.

849 Duan, A. M. and Wu G. X.: Weakening trend in the atmospheric heat source over the Tibetan Plateau during recent  
850 decades. Part I: Observations, *J. Clim.*, 21, 3149–3164, doi:10.1175/2007JCLI1912.1, 2008.

851 Flanner, M. G., Zender, C. S., Randerson, J. T., and Rasch, P. J.: Present day climate forcing and response from  
852 black carbon in snow, *J. Geophys. Res.*, 112, D11202, doi:10.1029/2006JD008003, 2007.

853 Flanner, M. G., Zender, C. S., Hess, P. G., Mahowald, N. M., Painter, T. H., Ramanathan, V., and Rasch, P. J.:  
854 Springtime warming and reduced snow cover from carbonaceous particles, *Atmos. Chem. Phys.*, 9, 2481–  
855 2497, doi:10.5194/acp-9-2481-2009, 2009.

856 Gettelman, A., Liu, X., Ghan, S. J., Morrison, H., Park, S., Conley, A. J., Klein, S. A., Boyle, J., Mitchell, D. L., and  
857 Li, J. L. F.: Global simulations of ice nucleation and ice supersaturation with an improved cloud scheme in  
858 the Community Atmosphere Model, *J. Geophys. Res.*, 115, D18216, doi:10.1029/2009jd013797, 2010.

859 Ginot, P., Dumont, M., Lim, S., Patris, N., Taupin, J.-D., Wagnon, P., Gilbert, A., Arnaud, Y., Marinoni, A.,  
860 Bonasoni, P., and Laj, P.: A 10 year record of black carbon and dust from a Mera Peak ice core (Nepal):  
861 variability and potential impact on melting of Himalayan glaciers, *The Cryosphere*, 8, 1479–1496,  
862 doi:10.5194/tc-8-1479-2014, 2014.

863 Hadley, O. L. and Kirchstetter, T.W.: Black-carbon reduction of snow albedo, *Nat. Clim. Change*, 2, 437–440, 2012.

864 Hall, D. K., Riggs G. A., and Salomonson V. V.: updated monthly. MODIS/TERRA Snow Cover Monthly L3  
865 Global 0.05Deg CMG V005, [2001], Boulder, CO, National Snow and Ice Data Center. Digital Media,  
866 distributed in netCDF format by the Integrated Climate Data Center (ICDC, <http://icdc.zmaw.de> University  
867 of Hamburg, Hamburg, Germany), 2006.

868 Hall, A. and Qu, X.: Using the current seasonal cycle to constrain snow albedo feedback in future climate change,  
869 *Geophys. Res. Lett.*, 33, L03502, doi:10.1029/2005GL025127, 2006.

870 Hansen, J. and Nazarenko, L.: Soot climate forcing via snow and ice albedos, *P. Natl. Acad. Sci. USA*, 101, 423–  
871 428, doi:10.1073/pnas.2237157100, 2004.

872 Hansen, J., Sato, M., Ruedy, R., Nazarenko, L., Lacis, A., Schmidt, G. A., Russell, G., Aleinov, I., Bauer, M., Bauer,  
873 S., Bell, N., Cairns, B., Canuto, V., Chandler, M., Cheng, Y., Del Genio, A., Faluvegi, G., Fleming, E.,  
874 Friend, A., Hall, T., Jackman, C., Kelley, M., Kiang, N., Koch, D., Lean, J., Lerner, J., Lo, K., Menon, S.,  
875 Miller, R., Minnis, P., Novakov, T., Oinas, V., Perlwitz, J., Perlwitz, J., Rind, D., Romanou, A., Shindell,  
876 D., Stone, P., Sun, S., Tausnev, N., Thresher, D., Wielicki, B., Wong, T., Yao, M., and Zhang, S.: Efficacy  
877 of climate forcings, *J. Geophys. Res.*, 110, D18104, doi:10.1029/2005JD005776, 2005.

878 Huang, J., Minnis, P., Yi, Y., Tang, Q., Wang, X., Hu, Y., Liu, Z., Ayers, K., Trepte, C., and Winker, D.: Summer  
879 dust aerosols detected from CALIPSO over the Tibetan Plateau, *Geophys. Res. Lett.*, 34, L18805,  
880 doi:10.1029/2007GL029938, 2007.

881 Huang, J., Fu, Q., Zhang, W., Wang, X., Zhang, R., Ye, H., and Warren, S. G.: Dust and black carbon in seasonal  
882 snow across Northern China, *Bull. Am. Meteorol. Soc.*, 92, 175–181, doi:10.1175/2010BAMS3064.1, 2011.

883 Hurrell, J. W., Holland, M. M., Ghan, S., Lamarque, J.-F., Lawrence, D., Lipscomb, W. H., Mahowald, N., Marsh,  
884 D., Rasch, P., Bader, D., Collins, W. D., Gent, P. R., Hack, J. J., Kiehl, J., Kushner, P., Large, W. G.,  
885 Marshall, S., Vavrus, S., and Vertenstein, M.: The Community Earth System Model: A Framework for  
886 Collaborative Research, *Bull. Am. Meteorol. Soc.*, 94, 1339–1360, doi:10.1175/BAMS-D-12-00121, 2013.

887 Immerzeel, W., VanBeek, L. P. H., and Bierkens, M. F. P.: Climate Change Will Affect the Asian Water Towers,  
888 *Science*, 328, 1382–1385, doi:10.1126/science.1183188, 2010.

889 | Jacobson, M. Z.: Climate response of fossil fuel and biofuel soot, accounting for soot's feedback to snow and sea ice  
890 albedo and emissivity, *J. Geophys. Res.*, 109, D21201, doi:10.1029/2004JD004945, 2004.

891 Jiao, C., Flanner, M. G., Balkanski, Y., Bauer, S. E., Bellouin, N., Bernsten, T. K., Bian, H., Carslaw, K. S.,  
892 Chin, M., De Luca, N., Diehl, T., Ghan, S. J., Iversen, T., Kirkevåg, A., Koch, D., Liu, X., Mann, G. W.,  
893 Penner, J. E., Pitari, G., Schulz, M., Seland, Ø., Skeie, R. B., Steenrod, S. D., Stier, P., Takemura, T.,  
894 Tsigaridis, K., van Noije, T., Yun, Y., and Zhang, K.: An AeroCom assessment of black carbon in Arctic  
895 snow and sea ice, *Atmos. Chem. Phys.*, 14, 2399–2417, doi:10.5194/acp-14-2399-2014, 2014.

896 Kang, S., Wake, C., Qin, D., Mayewski, P. A., and Yao, T.: Monsoon and dust signals recorded in Dasuopu glacier,  
897 Tibetan Plateau, *J. Glaciol.*, 46(153), 222–226, 2000.

898 Kang, S., Wei, X., You, Q., Flugel, W., Pepin, N., and Yao, T.: Review of climate and cryospheric change in the  
899 Tibetan Plateau, *Environ. Res. Lett.*, 5, 015101, doi:10.1088/1748-9326/5/1/015101, 2010.

900 Kaser, G., Grosshauser, M., and Marzeion, B.: Contribution of glaciers to water availability in different climate  
901 regimes, *P. Natl. Acad. Sci. USA*, 107, 20223–20227, doi:10.1073/pnas.1008162107, 2010.

902 Kaspari, S. D., Schwikowski, M., Gysel, M., Flanner, M. G., Kang, S., Hou, S., and Mayewski, P. A.: Resent  
903 increase in black carbon concentrations from a Mt. Everest ice core spanning 1860–2000 AD, *Geophys.*  
904 *Res. Lett.*, 38, L04703, doi:10.1029/2010GL046096, 2011.

905 Kopacz, M., Mauzerall, D. L., Wang, J., Leibensperger, E. M., Henze, D. K., and Singh, K.: Origin and radiative  
906 forcing of black carbon transported to the Himalayas and Tibetan Plateau, *Atmos. Chem. Phys.*, 11, 2837–  
907 2852, doi:10.5194/acp-11-2837-2011, 2011.

908 Lamarque, J.-F., Bond, T. C., Eyring, V., Granier, C., Heil, A., Klimont, Z., Lee, D., Liou, C., Mieville, A.,  
909 Owen, B., Schultz, M. G., Shindell, D., Smith, S. J., Stehfest, E., Van Aardenne, J., Cooper, O. R.,  
910 Kainuma, M., Mahowald, N., McConnell, J. R., Naik, V., Riahi, K., and van Vuuren, D. P.: Historical

Hailong Wang 4/5/2015 3:36 PM

**Deleted:** IPCC: Summary for Policymakers. In: Climate Change 2013: The Physical Science Basis. Contribution of Working Group I to the Fifth Assessment Report of the Intergovernmental Panel on Climate Change, edited by Stocker, T.F., Qin, D., Plattner, G.-K., Tignor, M., Allen, S.K., Boschung, J., Nauels, A., Xia, Y., Bex, V., and Midgley, P.M., Cambridge University Press, Cambridge, United Kingdom and New York, NY, USA, 2013.

(1850–2000) gridded anthropogenic and biomass burning emissions of reactive gases and aerosols: methodology and application, *Atmos. Chem. Phys.*, 10, 7017–7039, doi:10.5194/acp-10-7017-2010, 2010.

Lamarque, J. F., Emmons, L. K., Hess, P. G., Kinnison, D. E., Tilmes, S., Vitt, F., Heald, C. L., Holland, E. A., Lauritzen, P. H., Neu, J., Orlando, J. J., Rasch, P. J., and Tyndall, G. K.: CAM-chem: description and evaluation of interactive atmospheric chemistry in the Community Earth System Model, *Geosci. Model Dev.*, 5, 369–411, doi:10.5194/gmd-5-369-2012, 2012.

Lau, K. M., Kim, M. K., and Kim, K. M.: Asian monsoon anomalies induced by aerosol direct forcing: the role of the Tibetan Plateau, *Clim. Dyn.*, 26, 855–864, 2006.

Lau, K.-M., Kim, M. K., Kim, K.-M., and Lee, W. S.: Enhanced surface warming and accelerated snow melt in the Himalayas and Tibetan Plateau induced by absorbing aerosols, *Environ. Res. Lett.*, 5, 025204 doi:10.1088/1748-9326/5/2/025204, 2010.

Lee, Y. H., Lamarque, J.-F., Flanner, M. G., Jiao, C., Shindell, D. T., Bernsten, T., Bisiaux, M. M., Cao, J., Collins, W. J., Curran, M., Edwards, R., Faluvegi, G., Ghan, S., Horowitz, L. W., McConnell, J. R., Ming, J., Myhre, G., Nagashima, T., Naik, V., Rumbold, S. T., Skeie, R. B., Sudo, K., Takemura, T., Thevenon, F., Xu, B., and Yoon, J.-H.: Evaluation of preindustrial to present-day black carbon and its albedo forcing from Atmospheric Chemistry and Climate Model Intercomparison Project (ACCMIP), *Atmos. Chem. Phys.*, 13, 2607–2634, doi:10.5194/acp-13-2607-2013, 2013.

Li, X., Cheng, G., Jin, H., Kang, E., Che, T., Jin, R., Wu, L., Nan, Z., Wang, J., and Shen, Y.: Cryospheric change in China, *Global Planet. Change*, 62(3–4), 210–218, 2008.

Liu, X., Easter, R. C., Ghan, S. J., Zaveri, R., Rasch, P., Shi, X., Lamarque, J.-F., Gettelman, A., Morrison, H., Vitt, F., Conley, A., Park, S., Neale, R., Hannay, C., Ekman, A. M. L., Hess, P., Mahowald, N., Collins, W., Iacono, M. J., Bretherton, C. S., Flanner, M. G., and Mitchell, D.: Toward a minimal representation of aerosols in climate models: description and evaluation in the Community Atmosphere Model CAM5, *Geosci. Model Dev.*, 5, 709–739, doi:10.5194/gmd-5-709-2012, 2012.

Liu, Z., Liu, D., Huang, J., Vaughan, M., Uno, I., Sugimoto, N., Kittaka, C., Trepte, C., Wang, Z., Hostetler, C., and Winker, D.: Airborne dust distributions over the Tibetan Plateau and surrounding areas derived from the first year of CALIPSO lidar observations, *Atmos. Chem. Phys.*, 8, 5045–5060, doi:10.5194/acp-8-5045-2008, 2008.

Lu, Z., Streets, D. G., Zhang, Q., and Wang, S.: A novel back-trajectory analysis of the origin of black carbon transported to the Himalayas and Tibetan Plateau during 1996–2010, *Geophys. Res. Lett.*, 39, L01809, doi:10.1029/2011GL049903, 2012.

Ma, P.-L., Rasch, P. J., Wang, H., Zhang, K., Easter, R. C., Tilmes, S., Fast, J. D., Liu, X., Yoon, J.-H., and Lamarque, J.-F.: The role of circulation features on black carbon transport into the Arctic in the Community Atmosphere Model Version 5 (CAM5), *J. Geophys. Res. - Atmos.*, 118, 4657–4669, 2013.

Manabe, S., and Terpstra T. B.: The effects of mountains on the general circulation of the atmosphere as identified by numerical experiments, *J. Atmos. Sci.*, 31, 3–42, 1974.

Marinoni, A., Cristofanelli, P., Laj, P., Duchi, R., Calzolari, F., Decesari, S., Sellegri, K., Vuillermoz, E., Verza, G. P., Villani, P., and Bonasoni, P.: Aerosol mass and black carbon concentrations, a two year record at NCO-P (5079 m, Southern Himalayas), *Atmos. Chem. Phys.*, 10, 8551–8562, doi:10.5194/acp-10-8551-2010, 2010.

961 Marinoni, A., Cristofanelli, P., Laj, P., Duchi, R., Putero, D., Calzolari, F., Landi, T. C., Vuillermoz, E., Maione, M.,  
 962 and Bonasoni, P.: High black carbon and ozone concentrations during pollution transport in the Himalayas:  
 963 Five years of continuous observations at NCO-P global GAW station, *J. Environ. Sci.*, 25, 1618–1625,  
 964 doi:10.1016/S1001-0742(12)60242-3, 2013.

965 Ménégoz, M., Krinner, G., Balkanski, Y., Boucher, O., Cozic, A., Lim, S., Ginot, P., Laj, P., Gallée, H., Wagnon, P.,  
 966 Marinoni, A., and Jacobi, H. W.: Snow cover sensitivity to black carbon deposition in the Himalayas: from  
 967 atmospheric and ice core measurements to regional climate simulations, *Atmos. Chem. Phys.*, 14, 4237–  
 968 4249, doi:10.5194/acp-14-4237-2014, 2014.

969 Menon, S., Koch, D., Beig, G., Sahu, S., Fasullo, J., and Orlikowski, D.: Black carbon aerosols and the third polar  
 970 ice cap, *Atmos. Chem. Phys.*, 10, 4559–4571, doi:10.5194/acp-10-4559-2010, 2010.

971 Ming, J., Cachier, H., Xiao, C., Qin, D., Kang, S., Hou, S., and Xu, J.: Black carbon record based on a shallow  
 972 Himalayan ice core and its climatic implications, *Atmos. Chem. Phys.*, 8, 1343–1352, doi:10.5194/acp-8-  
 973 1343-2008, 2008.

974 Ming, J., Xiao, C. D., Cachier, H., Qin, D. H., Qin, X., Li, Z. Q., and Pu, J. C.: Black carbon (BC) in the snow of  
 975 glaciers in west China and its potential effects on albedos, *Atmos. Res.*, 92, 114–123,  
 976 doi:10.1016/j.atmosres.2008.09.007, 2009.

977 Ming, J., Xiao C., Sun J., Kang S., and Bonasoni P.: Carbonaceous particles in the atmosphere and precipitation of  
 978 the Nam Co region, central Tibet, *J. Environ. Sci.*, 22(11), 1748–1756, doi:10.1016/S1001-0742(09)60315-  
 979 6, 2010.

980 Ming, J., Xiao, C., Du, Z., and Yang, X.: An overview of black carbon deposition in High Asia glaciers and its  
 981 impacts on radiation balance, *Adv. Water Resour.*, 55, 80–87, 2013.

982 Moorthy, K. K., Beegum, S. N., Srivastava, N., Satheesh, S. K., Chin, M., Blond, N., Babu, S. S., and Singh, S.:  
 983 Performance evaluation of chemistry transport models over India, *Atmos. Environ.*, 71, 210–225, 2013.

984 Neale, R. B., Chen, C.-C., Gettelman, A., Lauritzen, P. H., Park, S., Williamson, D. L., Conley, A. J., Garcia, R.,  
 985 Kinnison, D., Lamarque, J.-F., Marsh, D., Mills, M., Smith, A. K., Tilmes, S., Vitt, F., Cameron-Smith, P.,  
 986 Collins, W. D., Iacono, M. J., Easter, R. C., Ghan, S. J., Liu, X., Rasch, P. J., and Taylor, M. A.:  
 987 Description of the NCAR Community Atmosphere Model (CAM 5.0), NCAR/TN-486+STR, available at:  
 988 [http://www.cesm.ucar.edu/models/cesm1.0/cam/docs/description/cam5\\_desc.pdf](http://www.cesm.ucar.edu/models/cesm1.0/cam/docs/description/cam5_desc.pdf) (last access: 26 December  
 989 2014), 2012.

990 Ohara, T., Akimoto, H., Kurokawa, J., Horii, N., Yamaji, K., Yan, X., and Hayasaka, T.: An Asian emission  
 991 inventory of anthropogenic emission sources for the period 1980–2020, *Atmos. Chem. Phys.*, 7, 4419–4444,  
 992 doi:10.5194/acp-7-4419-2007, 2007.

993 Petzold, A., Ogren, J. A., Fiebig, M., Laj, P., Li, S.-M., Baltensperger, U., Holzer-Popp, T., Kinne, S.,  
 994 Pappalardo, G., Sugimoto, N., Wehrli, C., Wiedensohler, A., and Zhang, X.-Y.: Recommendations for  
 995 reporting "black carbon" measurements, *Atmos. Chem. Phys.*, 13, 8365–8379, doi:10.5194/acp-13-8365-  
 996 2013, 2013.

997 Prasad, A. K. and Singh, R. P.: Changes in Himalayan Snow and Glacier Cover Between 1972 and 2000, *Eos Trans.*  
 998 *AGU*, 88, 33, doi:10.1029/2007EO330002, 2007.

999 Pu, Z., Xu L., and Salomonson V. V.: MODIS/Terra observed seasonal variations of snow cover over the Tibetan  
 1000 Plateau, *Geophys. Res. Lett.*, 34, L06706, doi:10.1029/2007GL029262, 2007.

Hailong Wang 4/5/2015 3:21 PM

**Deleted:** Menon, S., Hansen, J., Nazarenko, L.,  
 and Luo, Y.: Climate Effects of Black Carbon  
 Aerosols in China and India, *Science*, 297, 2250–  
 2253, doi:10.1126/science.1075159, 2002.

1005 Qian, Y., Flanner, M. G., Leung, L. R., and Wang, W.: Sensitivity studies on the impacts of Tibetan Plateau  
1006 snowpack pollution on the Asian hydrological cycle and monsoon climate, *Atmos. Chem. Phys.*, 11, 1929-  
1007 1948, doi:10.5194/acp-11-1929-2011, 2011.

1008 Qian, Y., Wang H., Zhang R., Flanner M. G., and Rasch P. J.: A sensitivity study on modeling black carbon in snow  
1009 and its radiative forcing over the Arctic and Northern China, *Environ. Res. Lett.*, 9, 064001,  
1010 doi:10.1088/1748-9326/9/6/064001, 2014.

1011 Qian, Y., Yasunari, T. J., Doherty, S. J., et al., Light-absorbing particles in snow and ice: measurement and  
1012 modeling of climatic and hydrological impact. *Adv. Atmos. Sci.*, 32(1), 64-91 doi: 10.1007/s00376-014-  
1013 0010-0, 2015.

1014 Qin, D., Liu, S., and Li, P.: Snow cover distribution, variability, and response to climate change in western China, *J.*  
1015 *Clim.*, 19(9), 1820–1833, 2006.

1016 Qiu, J.: China: the third pole. *Nature News*, 454(7203), 393-396, 2008.

1017 Ram, K., Sarin, M. M., and Hegde, P.: Long-term record of aerosol optical properties and chemical composition  
1018 from a high-altitude site (Manora Peak) in Central Himalaya, *Atmos. Chem. Phys.*, 10, 11791–11803,  
1019 doi:10.5194/acp-10-11791-2010, 2010.

1020 Ramanathan, V., Ramana, M. V., Roberts, G., Kim, D., Corrigan, C., Chung, C., Winker, D.: Warming trends in  
1021 Asia amplified by brown clouds solar absorption, *Nature*, 448, 575–578, 2007.

1022 Rasch, P. J., Mahowald, N. M., and Eaton, B. E.: Representations of transport, convection, and the hydrological  
1023 cycle in chemical transport models: Implications for the modeling of short-lived and soluble species, *J.*  
1024 *Geophys. Res.*, 102, 28 127–28 138, 1997.

1025 Ren, J., Jing, Z., Pu, J., and Qin, X.: Glaciers variations and climate change in the central Himalaya over the past  
1026 few decades, *Ann. Glaciol.*, 43, 218–222, 2006.

1027 Rienecker, M. M., Suarez, M. J., Gelaro, R., Todling, R., Bacmeister, J., Liu, E., Bosilovich, M. G., Schubert, S. D.,  
1028 Takacs, L., Kim, G.-K., Bloom, S., Chen, J., Collins, D., Conaty, A., da Silva, A., Gu, W., Joiner, J., Koster,  
1029 R. D., Lucchesi, R., and Molod, A.: MERRA – NASA’s Modern-Era Retrospective Analysis for Research  
1030 and Applications, *J. Clim.*, 24, 3624–3648, 2011.

1031 Singh, P. and Bengtsson, L.: Hydrological sensitivity of a large Himalayan basin to climate change, *Hydrol. Process.*,  
1032 18, 2363–2385, 2004.

1033 Taylor, K. E., Stouffer, R. J., and Meehl, G. A.: An Overview of CMIP5 and the Experiment Design, *Bull. Am.*  
1034 *Meteorol. Soc.*, 93, 485–498, doi:10.1175/BAMS-D-11-00094.1, 2012.

1035 Wang, B., Bao, Q., Hoskins, B., Wu, G., and Liu, Y.: Tibetan Plateau warming and precipitation changes in East  
1036 Asia, *Geophys. Res. Lett.*, 35, L14702, doi:10.1029/2008GL034330, 2008.

1037 Wang, H., Easter, R. C., Rasch, P. J., Wang, M., Liu, X., Ghan, S. J., Qian, Y., Yoon, J.-H., Ma, P.-L., and Vinoj, V.:  
1038 Sensitivity of remote aerosol distributions to representation of cloud–aerosol interactions in a global  
1039 climate model, *Geosci. Model Dev.*, 6, 765–782, doi:10.5194/gmd-6-765-2013, 2013.

1040 Wang, H., Rasch, P. J., Easter, R. C., Singh, B., Zhang, R., Ma, P. L., Qian, Y., and Beagley, N.: Using an explicit  
1041 emission tagging method in global modeling of source-receptor relationships for black carbon in the Arctic:

Variations, Sources and Transport pathways, *J. Geophys. Res.-Atmos.*, 119, 12888–12909, doi:10.1002/2014JD022297, 2014.

Wang, M., Xu, B., Cao, J., Tie, X., Wang, H., Zhang, R., Qian, Y., Rasch, P. J., Zhao, S., Wu, G., Zhao, H., Joswiak, D. R., Li, J., and Xie, Y.: Carbonaceous aerosols recorded in a southeastern Tibetan glacier: analysis of temporal variations and model estimates of sources and radiative forcing, *Atmos. Chem. Phys.*, 15, 1191–1204, doi:10.5194/acp-15-1191-2015, 2015.

Wang, X., S. J. Doherty, and J. Huang: Black carbon and other light-absorbing impurities in snow across Northern China, *J. Geophys. Res. Atmos.*, 118, 1471–1492, doi:10.1029/2012JD018291, 2013.

Warren, S. G. and Wiscombe, W. J.: A model for the spectral albedo of snow. II: Snow containing atmospheric aerosols, *J. Atmos. Sci.*, 37, 2734–2745, 1980.

Warren, S. G. and Wiscombe, W. J.: Dirty snow after nuclear war, *Nature*, 313, 469–470, 1985.

Wu, G., Liu, Y., He, B., Bao, Q., Duan, A., and Jin, F.-F.: Thermal controls on the Asian summer monsoon, *Sci. Rep.*, 2, 404, doi:10.1038/srep00404, 2012.

Xia, X. G., Zong, X. M., Cong, Z. Y., Chen, H. B., Kang, S. C., and Wang, P. C.: Baseline continental aerosol over the central Tibetan plateau and a case study of aerosol transport from South Asia, *Atmos. Environ.*, 45, 7370–7378, 2011.

Xu, B., Cao, J., Hansen, J., Yao, T., Joswiak, D. R., Wang, N., Wu, G., Wang, M., Zhao, H., Yang, W., Liu, X., and He, J.: Black soot and the survival of Tibetan glaciers, *Proc. Natl. Acad. Sci. USA*, 106, 22114–22118, 2009.

Xu, X., Lu C., Shi X., and Gao S.: World water tower: An atmospheric perspective, *Geophys. Res. Lett.*, 35, L20815, doi:10.1029/2008GL035867, 2008.

Yanai, M., Li, C., and Song, Z.: Seasonal heating of the Tibetan Plateau and its effects on the evolution of the Asian summer monsoon, *Journal of the Meteorological Society of Japan*, 70, 319–351, 1992.

Yao, T., Pu, J., Lu, A., Wang, Y., and Yu, W.: Recent glacial retreat and its impact on hydrological processes on the Tibetan Plateau, China, and surrounding regions, *Arct. Antarct. Alp. Res.*, 39(4), 642–650, 2007.

Yao, T., Thompson, L., Yang, W., Yu, W., Gao, Y., Guo, X., Yang, X., Duan, K., Zhao, H., Xu, B., Pu, J., Lu, A., Xiang, Y., Kattel, D. B., and Joswiak, D.: Different glacier status with atmospheric circulations in Tibetan Plateau and surroundings, *Nat. Clim. Change*, 2, 663–667, doi:10.1038/nclimate1580, 2012.

Yasunari, T. J., Bonasoni, P., Laj, P., Fujita, K., Vuillermoz, E., Marinoni, A., Cristofanelli, P., Duchi, R., Tartari, G., and Lau, K.-M.: Estimated impact of black carbon deposition during premonsoon season from Nepal Climate Observatory – Pyramid data and snow albedo changes over Himalayan glaciers, *Atmos. Chem. Phys.*, 10, 6603–6615, doi:10.5194/acp-10-6603-2010, 2010.

Ye, D. and Gao, Y.: *Meteorology of the Qinghai-Xizang Plateau* (Chinese Science Press, Beijing, 1979).

Ye, D. and Wu G.: The role of the heat source of the Tibetan Plateau in the general circulation, *Meteorol. Atmos. Phys.*, 67, 181–198, doi:10.1007/BF01277509, 1998.

Ye, H., Zhang, R., Shi, J., Huang, J., Warren, S. G., and Fu, Q.: Black carbon in seasonal snow across northern Xinjiang in northwestern China, *Environ. Res. Lett.* 7, 044002, doi:10.1088/1748-9326/7/4/044002, 2012.

Hailong Wang 3/31/2015 7:01 PM

**Deleted:** Wang, M., Xu, B., Cao, J., Tie, X., Wang, H., Zhang, R., Qian, Y., Rasch, P. J., Zhao, S., Wu, G., Zhao, H., Joswiak, D. R., Li, J., and Xie, Y.: Carbonaceous aerosols recorded in a Southeastern Tibetan glacier: variations, sources and radiative forcing, *Atmos. Chem. Phys. Discuss.*, 14, 19719–19746, doi:10.5194/acpd-14-19719-2014, 2014.

1087 Yeh, T., Lo, S., and Chu P.: The wind structure and heat balance in the lower troposphere over Tibetan Plateau and  
1088 its surrounding. *Acta Meteor. Sinica* 28, 108–121, 1957.

1089 Zhang, R., Hegg, D. A., Huang, J., and Fu, Q.: Source attribution of insoluble light-absorbing particles in seasonal  
1090 snow across northern China, *Atmos. Chem. Phys.*, 13, 6091–6099, doi:10.5194/acp-13-6091-2013, 2013.

1091 Zhang, X. Y., Arimoto, R., Cao, J. J., An, Z. S., and Wang, D.: Atmospheric dust aerosol over the Tibetan Plateau, *J.*  
1092 *Geophys. Res.*, 106(D16), 18 471–18 476, 2001.

1093 | Zhao, S., Ming, J., Xiao, C., Sun, W., and Qin, X.: A preliminary study on measurements of black carbon in the  
1094 atmosphere of northwest Qilian Shan. *J. Environ. Sci.*, 24(1), 152–159, doi:10.1016/S1001-0742(11)60739-  
1095 0, 2012.

1096 Zhao, Z., Cao, J., Shen, Z., Xu, B., Chen, L- W. A., Ho, K., Han, Y., Zhu, C., and Liu, S.: Aerosol particles at a  
1097 high-altitude site on the Southeast Tibetan Plateau, China: implications for pollution transport from South  
1098 Asia, *J. Geophys. Res.-Atmos.*, 118, 11360–11375, doi:10.1002/jgrd.50599, 2013.

Hailong Wang 4/5/2015 3:06 PM

**Deleted:** Zhao, L., Ping, C., Yang, D., Cheng, G., Ding, Y., and Liu, S.: Changes of climate and seasonally frozen ground over the past 30 years in Qinghai-Xizang (Tibetan) Plateau, China, *Global Planet. Change*, 43, 19–31, 2004. -

1099 |



**Table 1.** List of sites for the observations of atmospheric BC surface concentrations used in this study to evaluate our model simulation.

Site	Latitude (°N)	Longitude (°E)	Elevation (m)		Sampling time	Observation method	Contributor
			observation	model			
<b>Muztagh Ata</b>	38.3	75.0	4500	3497	2003–2006	Thermal Optical Reflectance (TOR)	Cao et al., 2009
<b>Hanle</b>	32.8	79.0	4250	4862	2009–2010	Aethalometer	Babu et al., 2011
<b>Manora Peak</b>	29.4	79.5	1950	1409	2005–2008	Thermal Optical Transmittance (TOT)	Ram et al., 2010
<b>NCO-P</b>	28.0	86.8	5079	4604	2006–2008	Multi-angle absorption photometer (MAAP)	Marinoni et al., 2010
<b>Lulang</b>	29.5	94.4	3300	3370	2008–2009	TOR	Zhao et al., 2013
<b>NCOS</b>	30.8	91.0	4730	4956	2006–2007	TOR	Ming et al., 2010
<b>QSSGEE</b>	39.5	96.5	4214	2748	2009–2011	Aethalometer	Zhao et al., 2012

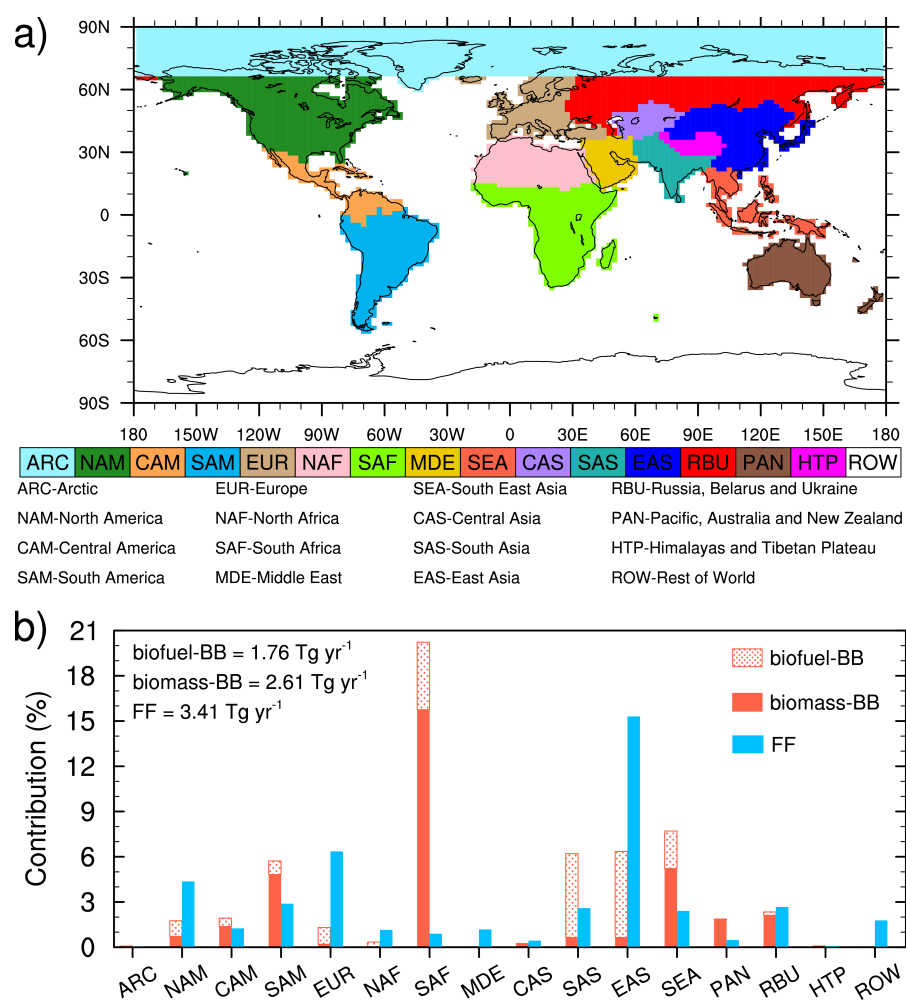


**Fig. 1.** (a) Tagged source regions and (b) the respective percentage contributions to global annual mean BC emissions from the individual source regions and sectors (including biofuel, biomass burning and fossil fuel). The global annual mean BC emission rate is 7.78 Tg yr<sup>-1</sup>, which is divided up into the three sectors as indicated by the numbers at the upper-left corner.

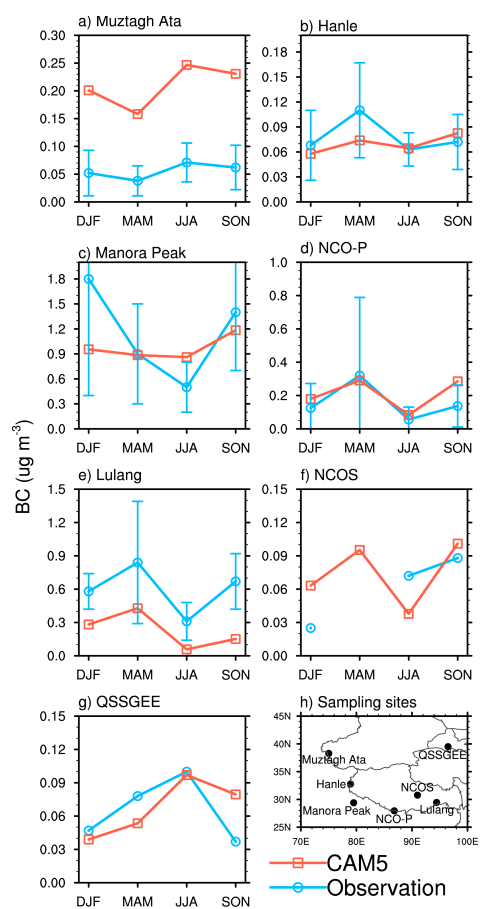


**Fig. 2.** Seasonal mean surface BC concentration ( $\mu\text{g m}^{-3}$ ) from observations (blue lines with error bars denoting SD) and CAM5 simulation (red lines) at the seven sampling sites listed in Table 1 and marked in map of panel h.

Hailong Wang 3/29/2015 8:48 PM

Deleted: aerosol

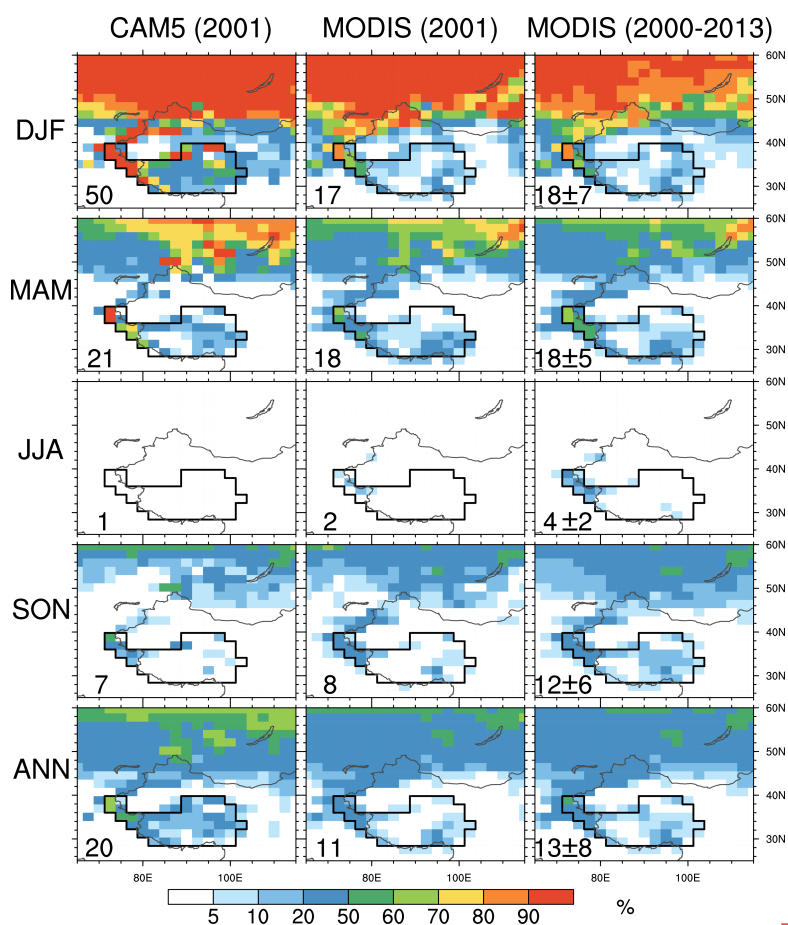


**Fig. 3.** Seasonal and annual mean snow cover fraction from CAM5 simulation for year 2001 (left), and MODIS retrieval for 2001 (middle) and 2000-2013 (right). The summer (JJA) in 2001 for both CAM5 and MODIS only includes July and August due to missing MODIS data in June.

The number in the lower-left corner of each panel is the corresponding spatial mean SCF for the HTP region (which is marked with black outline), and for MODIS the standard deviation calculated from the MODIS multi-year means is also included.

Hailong Wang 3/31/2015 5:12 PM

CAM5 (2001)

DJF

MAM

JJA

SON

ANN

Deleted:

Hailong Wang 3/31/2015 5:16 PM

Deleted: T

Hailong Wang 3/31/2015 5:17 PM

Deleted: is

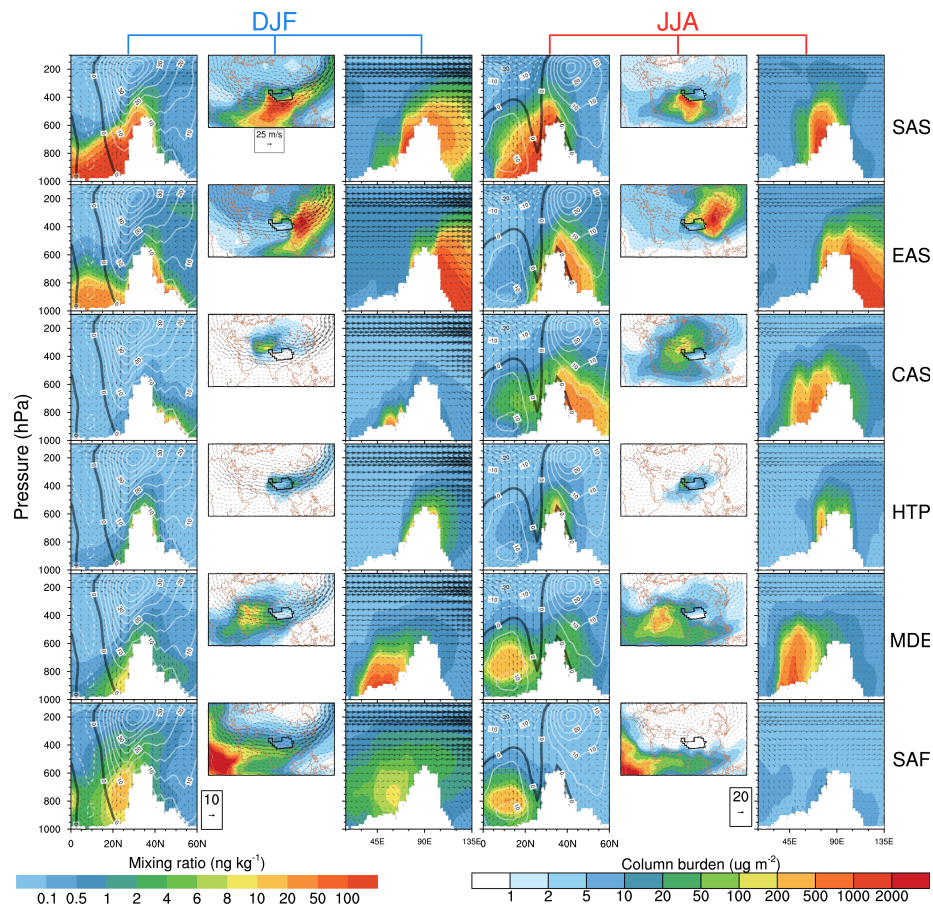


**Fig. 4.** The first column shows the latitude-height distributions of DJF BC mass mixing ratios (in  $\text{ng kg}^{-1}$ , colors) averaged over  $71.25\text{--}101.25^\circ\text{E}$ , originating from BB and FF sectors in the tagged source regions (corresponding to different rows); the white shaded area denotes topography, and the superimposed white contours at intervals of  $5 \text{ m s}^{-1}$  represent the westerly (solid) and easterly (dashed) DJF mean zonal winds along the cross-section with the thick solid black contour at  $0 \text{ m s}^{-1}$ ; the wind vectors (consisting of vertical velocity in units of  $-10^{-4} \text{ hPa s}^{-1}$  and meridional wind in  $\text{m s}^{-1}$ ) are represented by arrows. Colors in the second column denote spatial distribution of the DJF mean BC column burden (in  $\mu\text{g m}^{-2}$ ), originating from different source regions, and the arrows represent the DJF mean horizontal wind vectors at 500hPa; the HTP is marked with black outline. The third column is similar to the first column except that the quantities are on the longitude-height cross-section averaged over  $28\text{--}40^\circ\text{N}$ , and thus the horizontal component of the wind vectors is zonal wind ( $\text{m s}^{-1}$ ) instead. The fourth to sixth columns are the same as the first to third columns, respectively, but for JJA means instead.

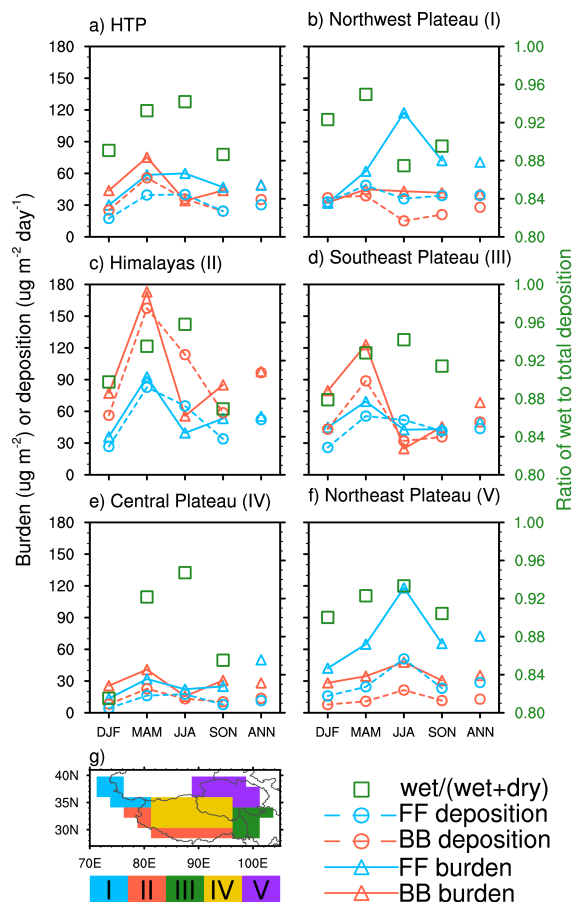


**Fig. 5.** Seasonal and annual mean BC column burden (solid lines and open triangles, in  $\mu\text{g m}^{-2}$ ) and deposition rate (dashed lines and open circles, in  $\mu\text{g m}^{-2} \text{ day}^{-1}$ ) over (a) the HTP, (b) Northwest Plateau, (c) Himalayas, (d) Southeast Plateau, (e) Central Plateau and (f) Northeast Plateau, emitted from BB (red color) and FF (blue color) source sectors. The green squares denote the ratio of wet to total BC deposition (using y-axis on the right) in four seasons over each receptor region. The geographical locations of five sub-regions of HTP are indicated in panel g.

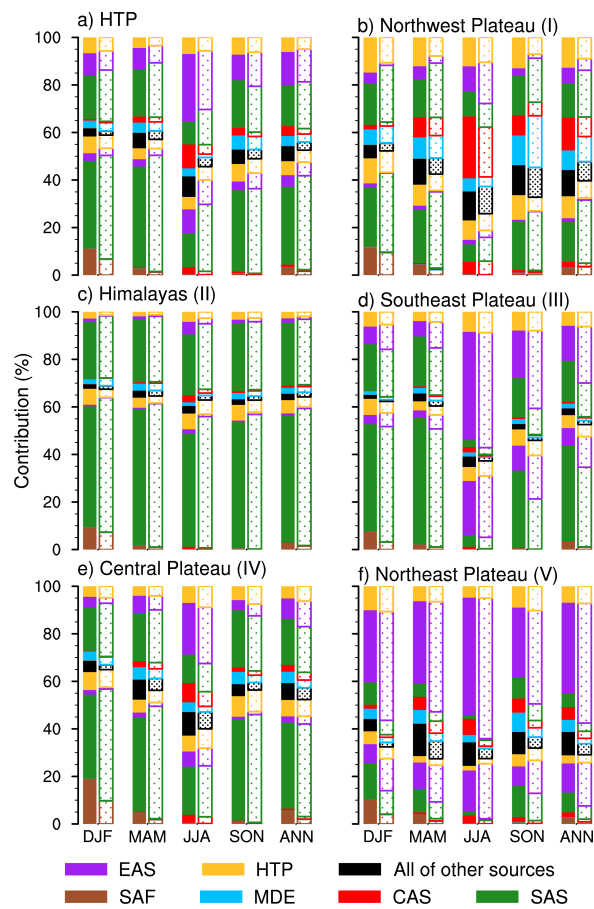


**Fig. 6.** Fractional contributions (measured by the lengths of color bars) to seasonal and annual mean BC column burden (solid pattern bars) and deposition (dotted pattern bars) over (a) the HTP, (b) Northwest Plateau, (c) Himalayas, (d) Southeast Plateau, (e) Central Plateau, and (f) Northeast Plateau, originating from six major tagged source regions (indicated by colors at the bottom) for BB (colors below the black bar) and FF (colors above the black color) emissions. The black bar in each column represents the contribution from all of the other tagged source regions and sectors.

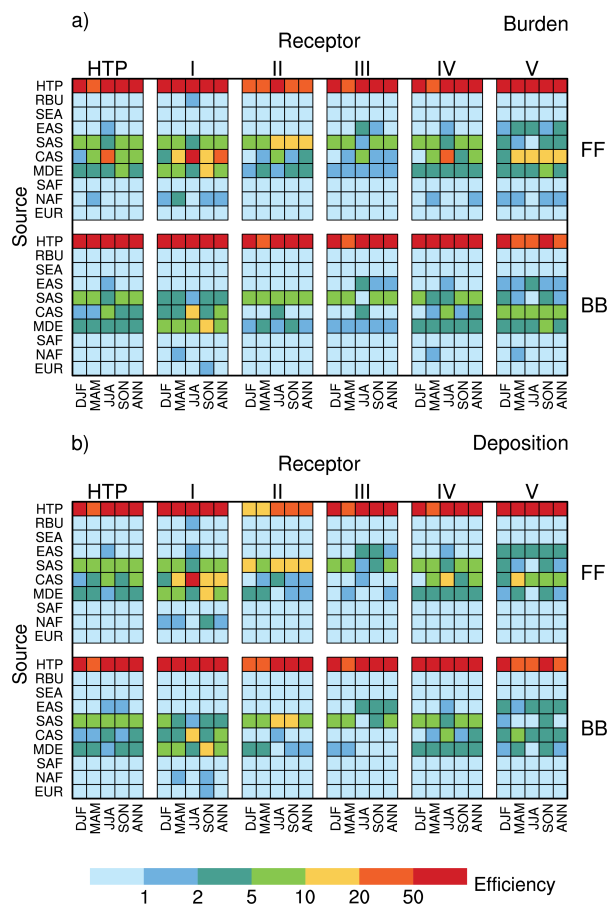


**Fig. 7.** Efficiency of FF (top) and BB (bottom) emissions from ten source regions (on the y-axis) in changing seasonal and annual mean (a) BC column burden and (b) deposition over the HTP and each of the five sub-regions: Northwest Plateau (I), Himalayas (II), Southeast Plateau (III), Central Plateau (IV) and Northeast Plateau (V).



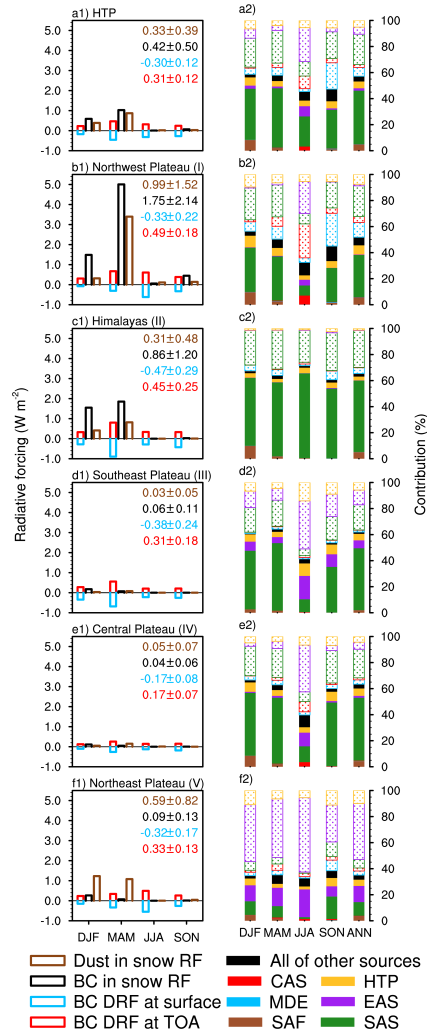


**Fig. 8.** Seasonal mean radiative forcing (left column) induced by the various BC effects (indicated by the color legend at the bottom) and dust-in-snow effect over (a1) the HTP, (b1) Northwest Plateau, (c1) Himalayas, (d1) Southeast Plateau, (e1) Central Plateau and (f1) Northeast Plateau. The corresponding annual mean forcings and one SD (for 12 monthly means) are shown in numbers on the top-right corner of each panel. The right column (a2-f2) panels represent source contribution to surface BC-in-snow radiative forcing over the corresponding receptors from tagged source regions (colors) and sectors (solid pattern bar and dotted pattern bar for BB and FF, respectively). The black bar in each column represents the contribution from all of the other tagged source regions and sectors.